BINARY BLACK HOLE MERGERS FROM THE FIRST STARS: ROLES PLAYED BY TWO EVOLUTION CHANNELS

Boyuan Liu[1,2]

Collaborators: Tilman Hartwig, Nina S. Sartorio, Irina Dvorkin, Guglielmo Costa, Filippo Santoliquido, Anastasia Fialkov, Ralf S. Klessen, Volker Bromm, Michela Mapelli

(for details, see **arXiv:2406.17397** and *https://gitlab.com/Treibeis/a-sloth-cob*)

[1] *Institute of Astronomy, University of Cambridge*
[2] *Zentrum für Astronomie der Universität Heidelberg*

First stars: Population III (Pop III)

Pop III stars[1]**: massive** ($\sim 10 - 1000\ \mathrm{M}_\odot$) **stars formed in minihaloes** ($M_\mathrm{h} \sim 10^{5-8}\ \mathrm{M}_\odot$) **at** $z \sim 10 - 30$ via collapse of primordial ($Z \lesssim 10^{-6}\ \mathrm{Z}_\odot$) gas cooled by H_2 (and HD)

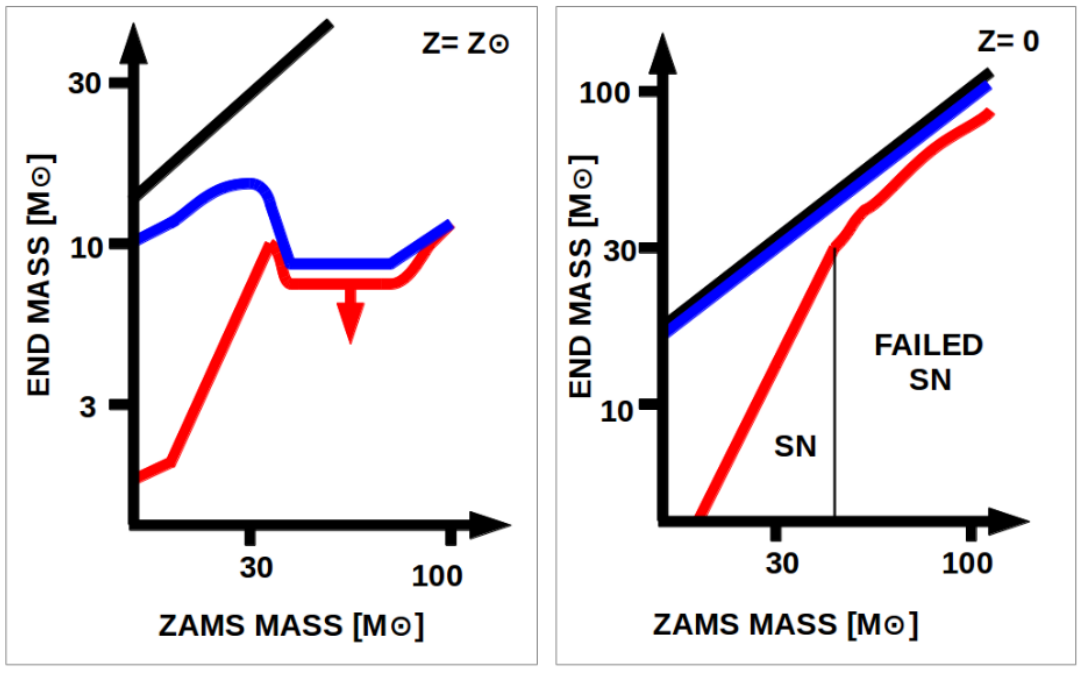

(Mapelli, 2020)

Pop III stars are more likely to become massive black holes (BHs) than present-day stars.$\rightarrow$ binary BH (BBH) mergers

Gravitational waves (GWs) can be a promising probe of Pop III stars

(see, e.g., Iwaya et al., 2023; Franciolini et al., 2024; Santoliquido et al., 2024).

[1] Direct observations of the light from individual Pop III stars are still challenging: *We need a 100-meter infrared telescope on the moon (Schauer et al., 2020).*

Binaries of Pop III stars: theoretical challenge

‘Standard’ picture of Pop III star formation from simulations:
Pop III stars typically form in small clusters.

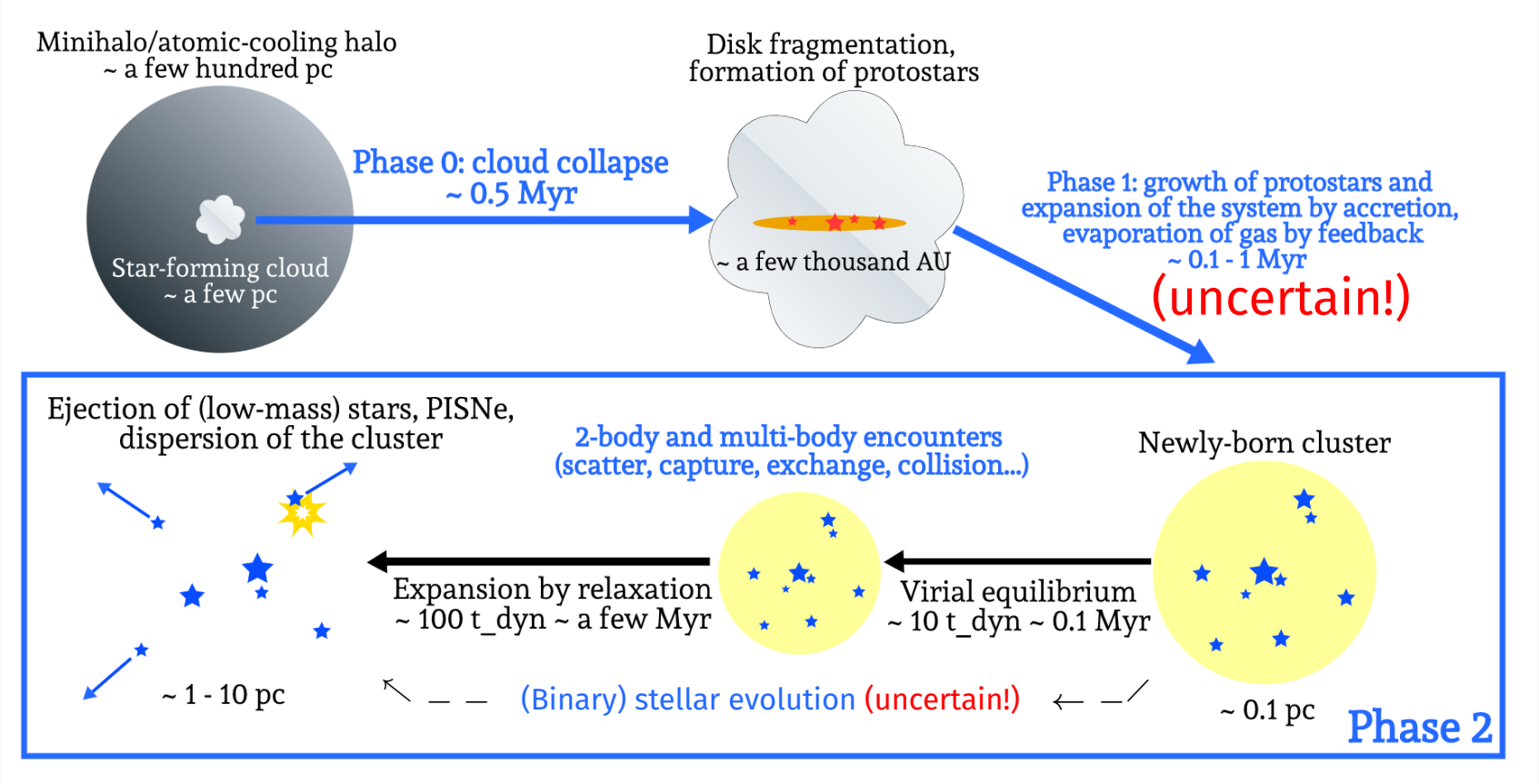

Due to computational limitations, the detailed evolution from initial protostar formation and growth to ‘dry’ star clusters is still unclear.

Pop III BBH mergers from isolated evolution

Limitations of the isolated binary stellar evolution (IBSE) channel:

- **Significant uncertainties in the initial condition and binary stellar evolution parameters lead to large discrepancies in the predictions from different models, with ~ 3 (5) orders of magnitude of scatter in the peak (local) merger rate density.**
- **The IBSE channel only works for initially close ($\lesssim 10$ AU) binary stars.** However, recent hydrodynamic and N-body simulations indicate that **close binaries of Pop III stars are likely rare** ($\lesssim 2\%$) due to expansion of protostar clusters/binaries by accretion of in-falling gas with high angular momentum (Susa, 2019; Sugimura et al., 2020, 2023; Liu et al., 2021; Park et al., 2023, 2024).

New channels for Pop III BBH mergers?

Dynamical hardening (DH) by 3-body encounters

Heggie-Hills Law: Soft binaries soften, and hard binaries harden.
(Hard: binding energy > average kinetic energy of surrounding objects)

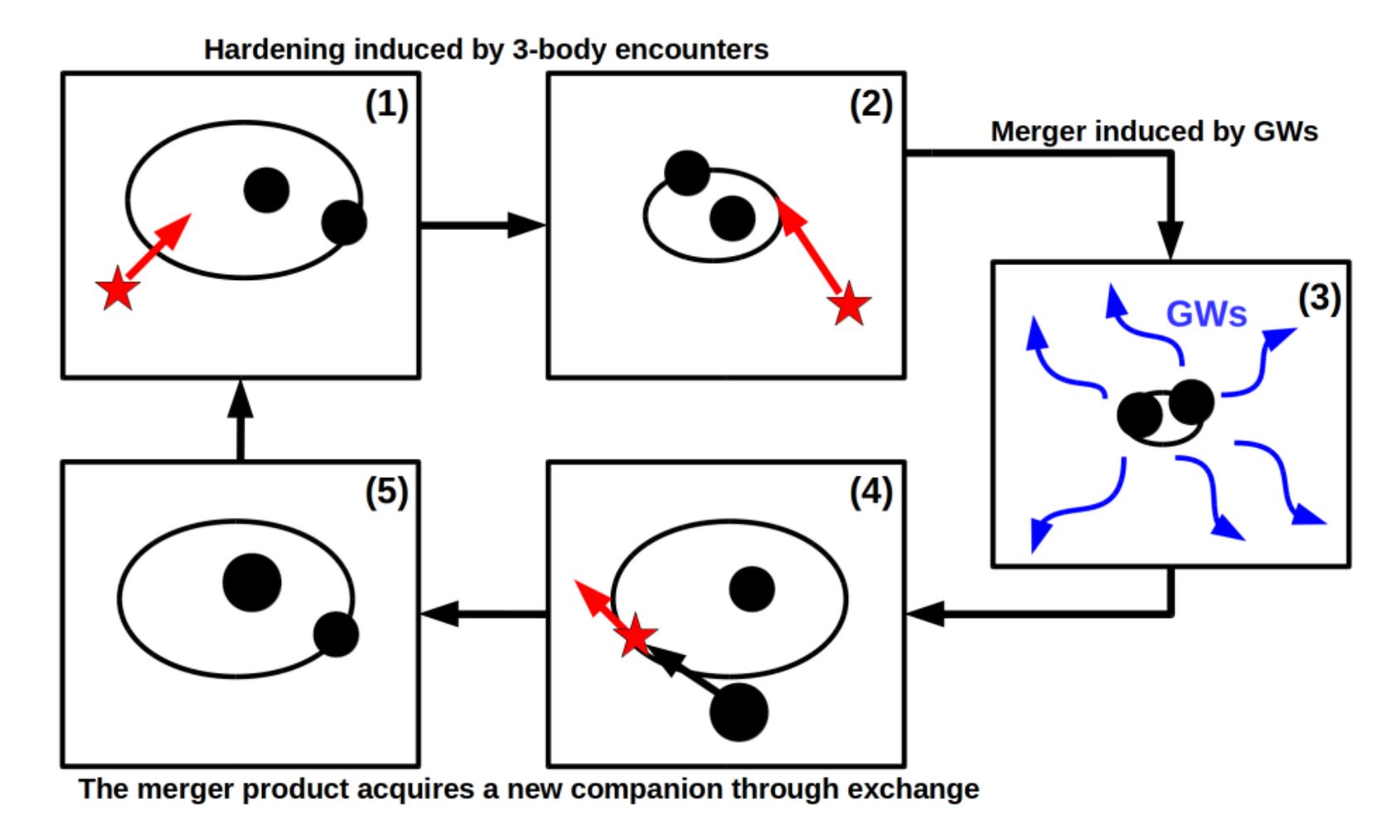

(Mapelli, 2020)

Pop III BBH mergers in nuclear star clusters (NSCs)

The NSC-DH channel (Liu & Bromm, 2021):
Dynamics of Pop III BBHs within galaxies and during halo mergers → infall into NSCs by dynamical friction →
evolution in NSCs (disruptions, ejections, hardening) → BBH mergers

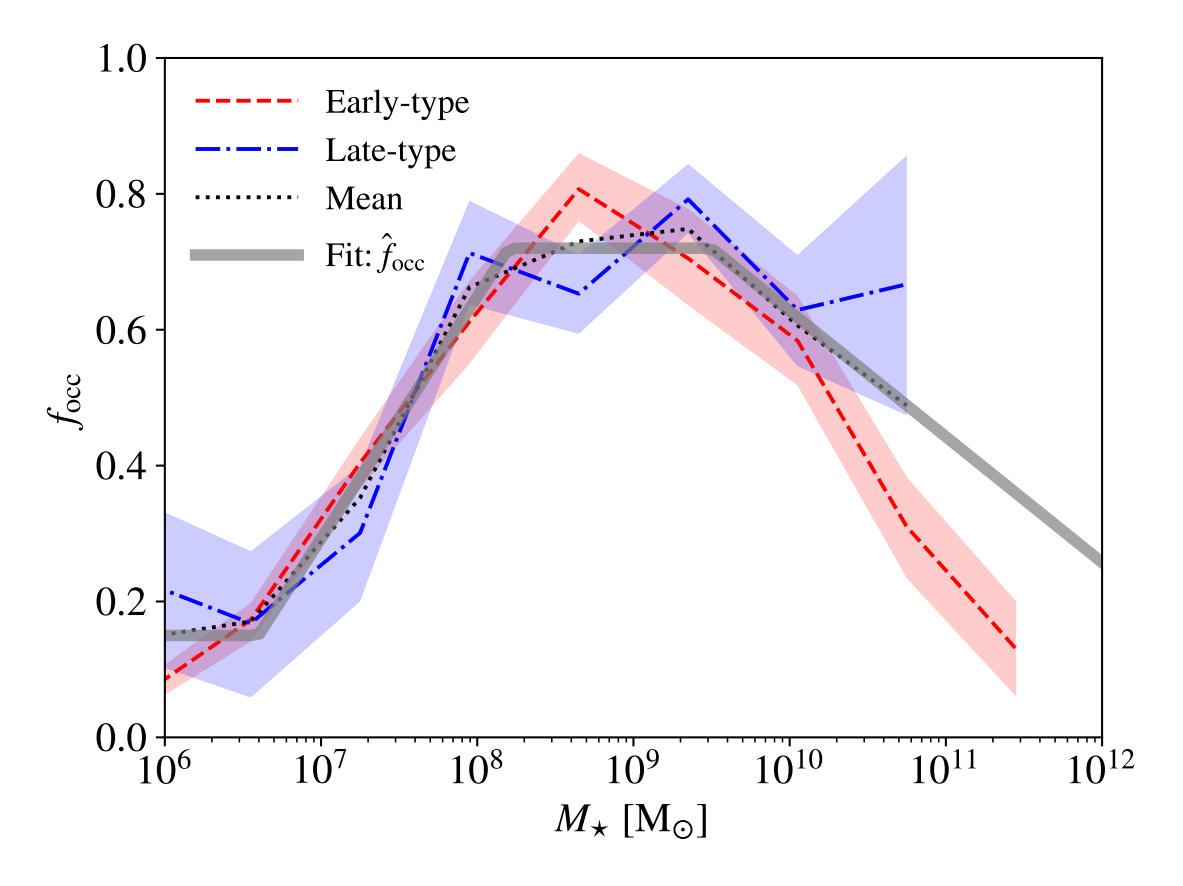

In-situ dynamical channel: Non-standard pathways of Pop III star formation (in more massive atomic-cooling halos under peculiar conditions) tend to produce massive ($\gtrsim 10^4$ $M_\odot$) clusters of Pop III stars, where dynamical interactions also play important roles in BBH evolution (Wang et al., 2022; Liu et al., 2023a; Mestichelli et al., 2024).

Two channels in one framework

Aim: understand the relative importance and unique features of the NSC-DH and IBSE channels under various assumptions on Pop III binary stars and high-z NSCs.

- Semi-analytical model **A-SLOTH** (Hartwig et al., 2022) for **Pop III and Pop I/II star formation and stellar feedback along halo merger trees** from the cosmological simulation by Ishiyama et al. (2016) with parameters calibrated to observations → Pop III star formation $\delta M_{\star,\mathrm{III}}$, halo mergers, galaxy mass $M_\star$
- Stochastic sampling of Pop III BBHs based on the **binary population synthesis (BPS) results from SEVN (Costa et al., 2023)** given $\delta M_{\star,\mathrm{III}}$
- Initialization and randomization of the galactic orbits of Pop III BBHs (during formation and halo mergers) with the spatial distribution of Pop III remnants in halos predicted by cosmological hydrodynamic simulations (Liu & Bromm, 2020a,b)
- Galaxy and NSC models based on empirical scaling relations for mass, size, compactness, and occupation fraction (Portegies Zwart et al., 2010; Arca-Sedda & Capuzzo-Dolcetta, 2014; Neumayer et al., 2020; Behroozi et al., 2019) given $M_\star$
- Evolution of external/galactic and internal orbits of Pop III BBHs in galaxy fields (IBSE) and NSCs (NSC-DH) → BBH mergers and host system properties
- **See more details in Liu et al. (2024), code available at *https://gitlab.com/Treibeis/a-sloth-cob***

Predictions: merger rate density (MRD), stochastic GW background (SGWB), detection rates by the LVK and ET, BH mass distribution

Parameters explored ($3 \times 2 \times 3 = 18$ models)

(a) Initial mass function (IMF) for primary stars (m_1)

- LOG (log-flat): $p(m_1) \propto m_1^{-1}$ *(fiducial)*
- TOP (top-heavy): $p(m_1) \propto m_1^{-0.17} \exp[-(20\ \mathrm{M}_\odot^2)/m_1^2]$
- KRO (bottom-heavy): $p(m_1) \propto m_1^{-2.3}$

(b) **Initial binary statistics (IBS): period (P), eccentricity (e), and mass ratio (q)**

- **S12 (denoted by '1', dominated by close binaries):** $p(\pi) \propto \pi^{-0.55}$ **for** $\pi \in [0.15, 5.5]$, $p(e) \propto e^{-0.42}$, $p(q) \propto q^{-0.1}$ **(Sana et al., 2012)** ***(fiducial)***
- **SB13 (denoted by '5', dominated by wide binaries):** $p(\pi) \propto \exp[-0.36(\pi - 5.5)^2]$, $p(e) = 2e$, $p(q) \propto q^{-0.55}$ **(Stacy & Bromm, 2013)**

$\pi \equiv \log(P/\mathrm{day})$, see Sec. 2.3 of Costa et al. (2023) for details

(c) NSC occupation fraction f_{occ} as a function of galaxy mass $M_\star$

- obs (empirical): $f_{\mathrm{occ}} = \hat{f}_{\mathrm{occ}}(M_\star)$, $M_{\star,\mathrm{min}} = 10^6\ \mathrm{M}_\odot$ *(fiducial)*
- full (optimistic): $f_{\mathrm{occ}} = 1$, $M_{\star,\mathrm{min}} = 10^6\ \mathrm{M}_\odot$ (Leaman & van de Ven, 2022)
- low (conservative): $f_{\mathrm{occ}} = \hat{f}_{\mathrm{occ}}(M_\star)$, $M_{\star,\mathrm{min}} = 10^{10}\ \mathrm{M}_\odot$ for $z > 5$ (Ma et al., 2021)

$\hat{f}_{\mathrm{occ}}(M_\star)$: fit to observations (Neumayer et al., 2020), $f_{\mathrm{occ}} = 0$ for $M_\star < M_{\star,\mathrm{min}}$

Fixed parameters: primary mass range: $m_1 \in [5, 550]\ \mathrm{M}_\odot$, secondary mass range: $m_2 \in [2.2, 550]\ \mathrm{M}_\odot$, mass ratio range: $q \in [0.1, 1]$. A-SLOTH (best-fit) parameters for star formation and stellar feedback (see table 1 of Hartwig et al. 2022), DH efficiency, parameters of the galaxy and NSC models, binary stellar evolution parameters in SEVN

Initial condition models (Costa et al., 2023)

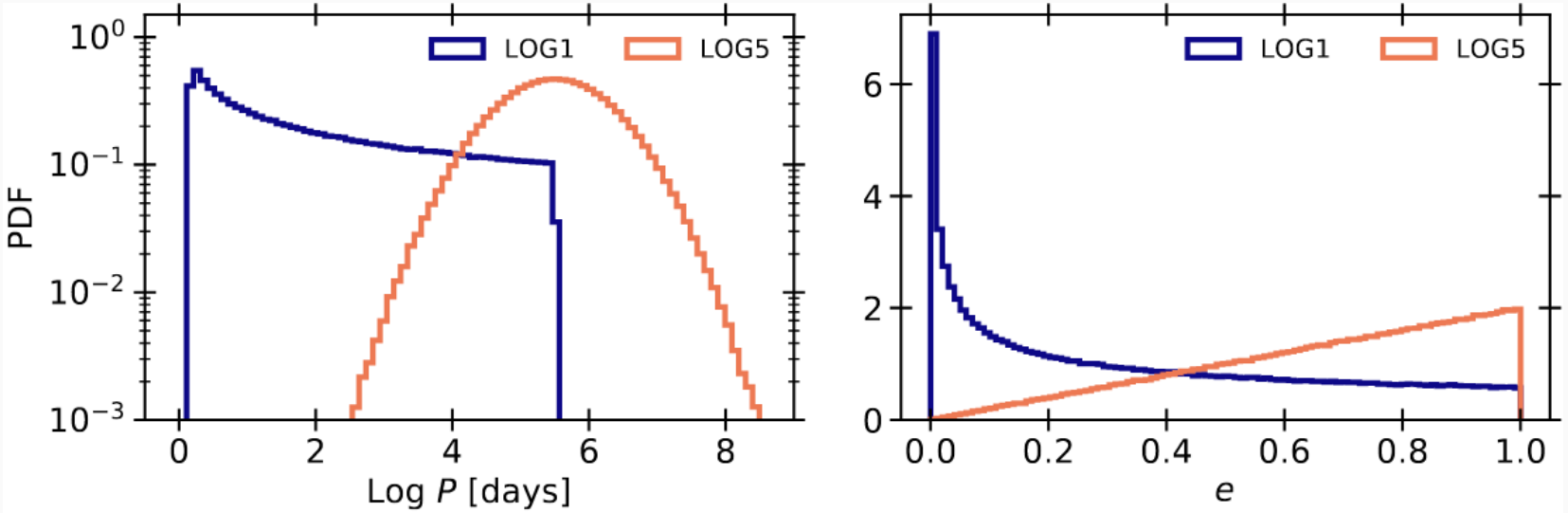

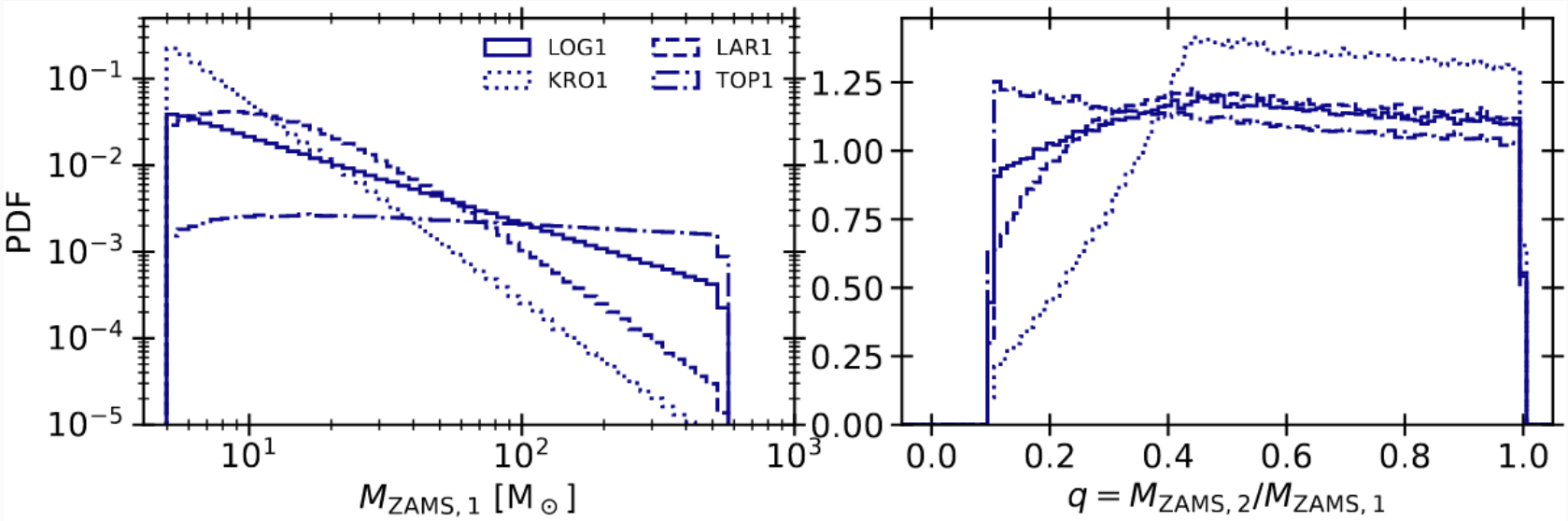

Impact of IBS on MRD

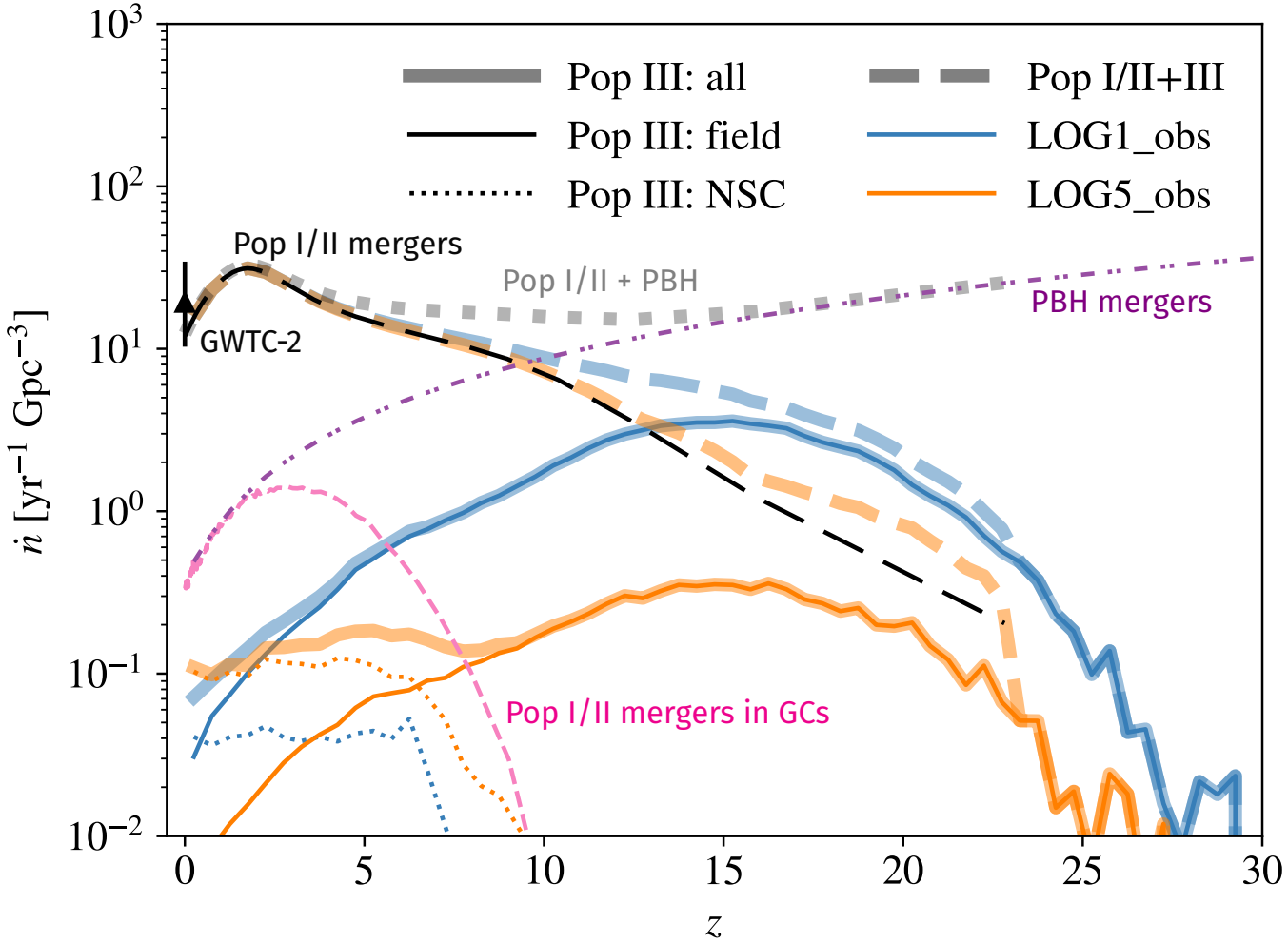

Local BBH MRD inferred from the GWTC-2 events: $\dot{n}_{\rm obs}(z\sim 0) = 19.3^{+15.1}_{-9}\ {\rm yr}^{-1}\ {\rm Gpc}^{-3}$ (Abbott et al., 2021). The results for Pop I/II and PBH mergers are taken from Franciolini et al. (2022). The IMF and NSC parameters are fixed to the fiducial choices ('LOG' and 'obs').

Impact of IBS on SGWB

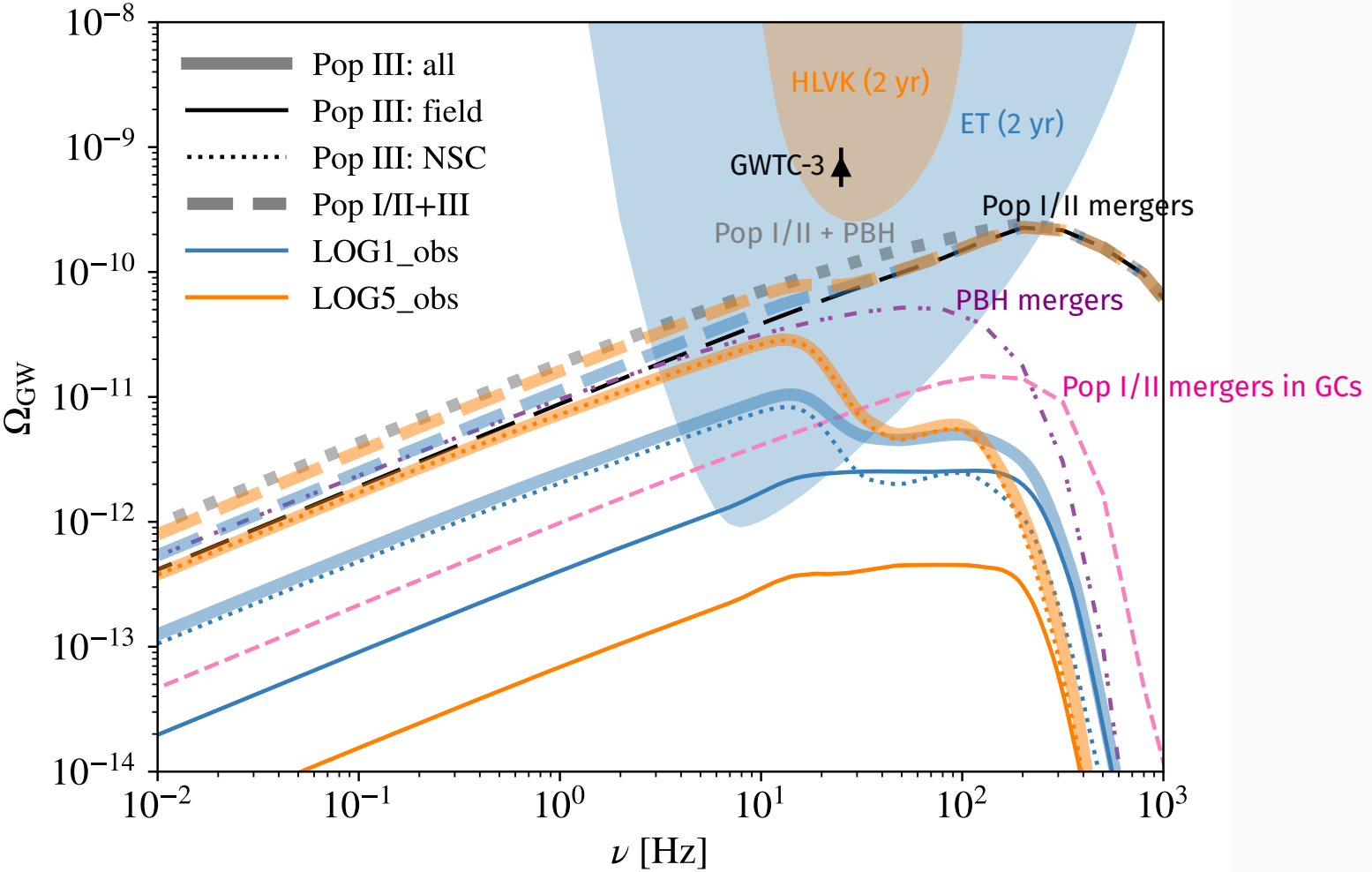

Total SGWB inferred from GWTC-3 events: $\Omega_{\rm GW}(f = 25\ {\rm Hz}) = 6.9^{+3.0}_{-2.1} \times 10^{-10}$ (Abbott et al., 2023). The conservative results for Pop I/II and PBH mergers and detector sensitivity curves are taken from Bavera et al. (2022). The IMF and NSC parameters are fixed to the fiducial choices.

Difference between the two channels: progenitor

Initial pericenter distance ($r_{\rm p}$) distribution for LOG5_obs:

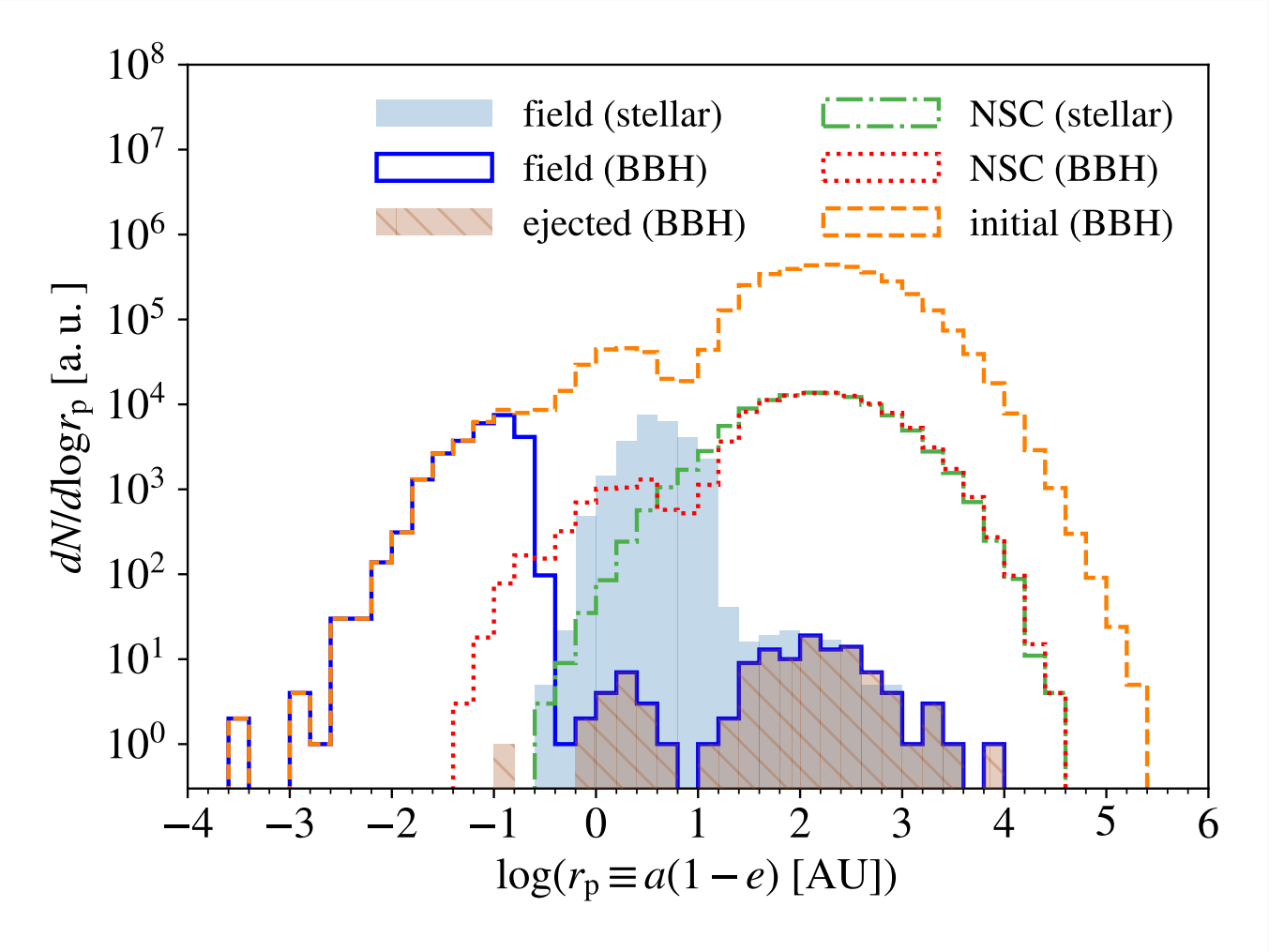

The NSC-DH channel is also effective for initially wide binary stars and BBHs with pericenter distances up to $\sim 10^5$ AU!

Difference between the two channels: chirp mass

Chirp mass distribution (normalized) of BBH mergers for LOG5_obs:

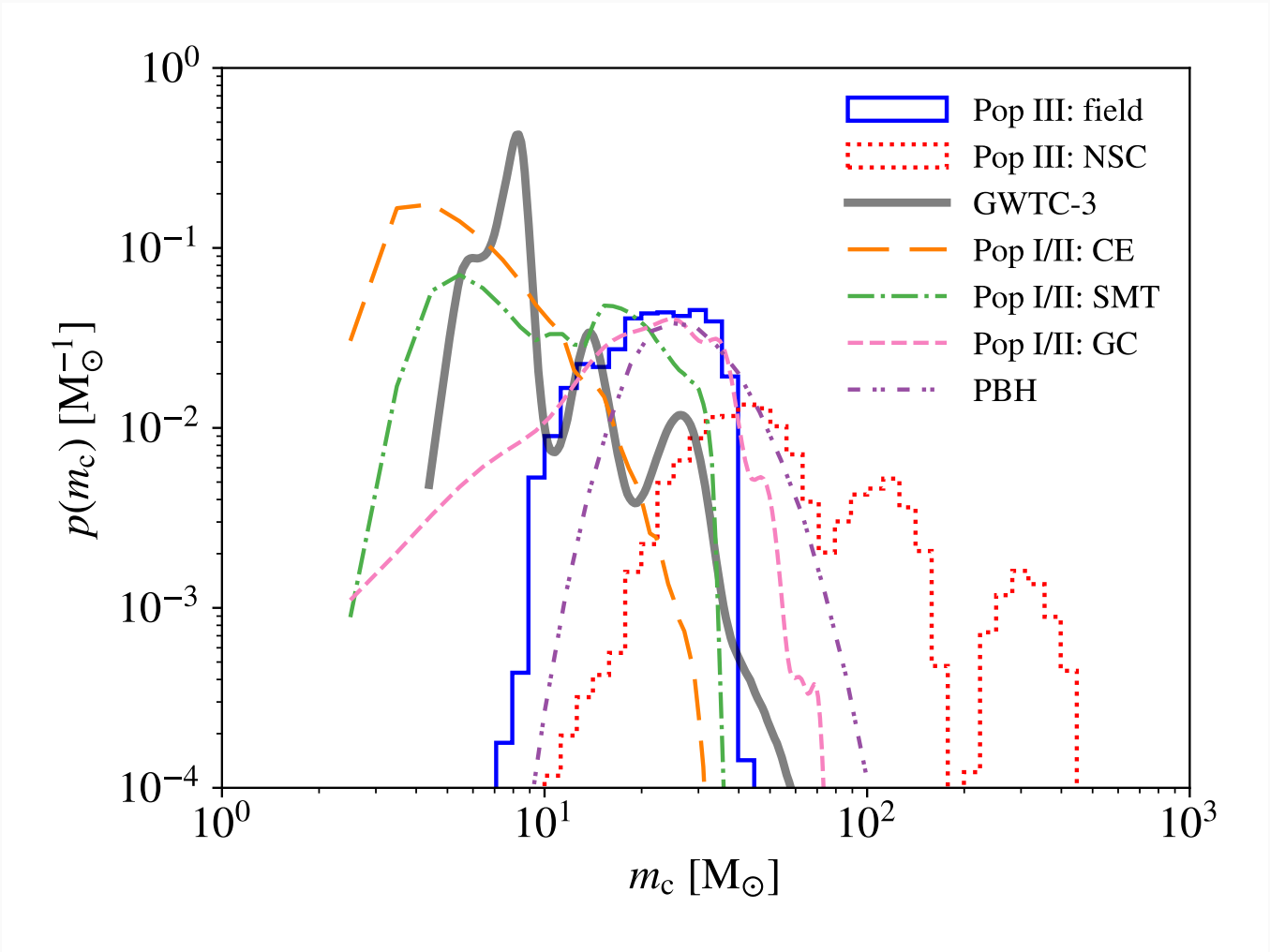

The thick solid curve shows the intrinsic chirp mass distribution inferred from GWTC-3 events (Abbott et al., 2023). The results for Pop I/II mergers from various channels and PBH mergers are taken from Franciolini et al. (2022). Massive BBH mergers can also be produced by IBSE in other binary stellar evolution models (Tanikawa et al., 2021a,b, 2022; Hijikawa et al., 2021; Santoliquido et al., 2023; Mestichelli et al., 2024; Tanikawa, 2024).

Detection rates by ET (SNR>8)

- All mergers: $\dot{\mathcal{N}}_{\rm ET,SNR>8} \sim 50 - 1370\ {\rm yr}^{-1}$ in total,
  $\sim 6 - 230\ {\rm yr}^{-1}$ for NSC mergers, and $\sim 30 - 1230\ {\rm yr}^{-1}$ for field mergers
- Intermediate-mass BH (IMBH) mergers ($m_1 > 100\ {\rm M}_\odot$):
  $\dot{\mathcal{N}}_{\rm ET,IMBH,SNR>8} \sim 0.5 - 200\ {\rm yr}^{-1}$ in NSCs and $\lesssim 0.1\ {\rm yr}^{-1}$ in galaxy fields
- Fraction in NSCs:
  $\mathcal{F}_{\rm NSC} \sim 1 - 22\%$ for S12 (close binaries) and $\sim 13 - 88\%$ for SB13 (wide binaries)

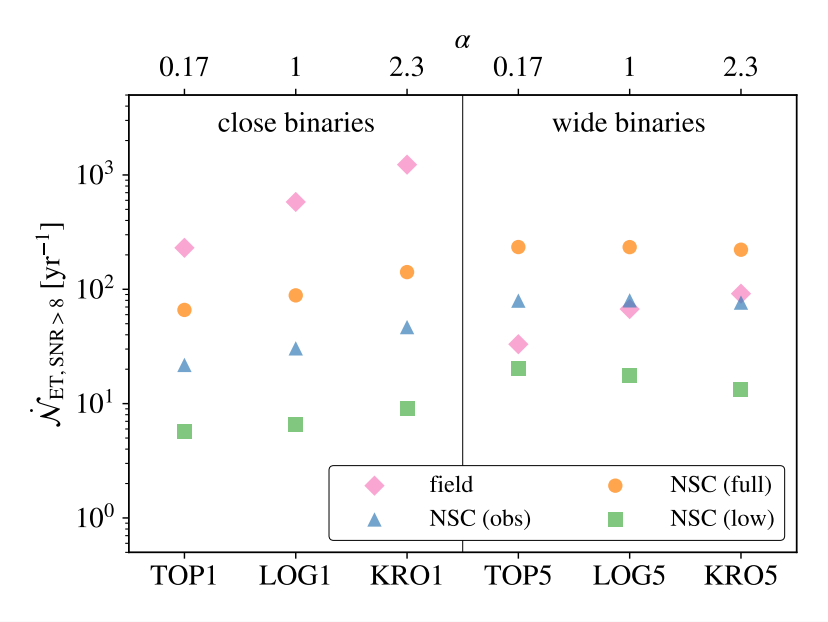

(all mergers)

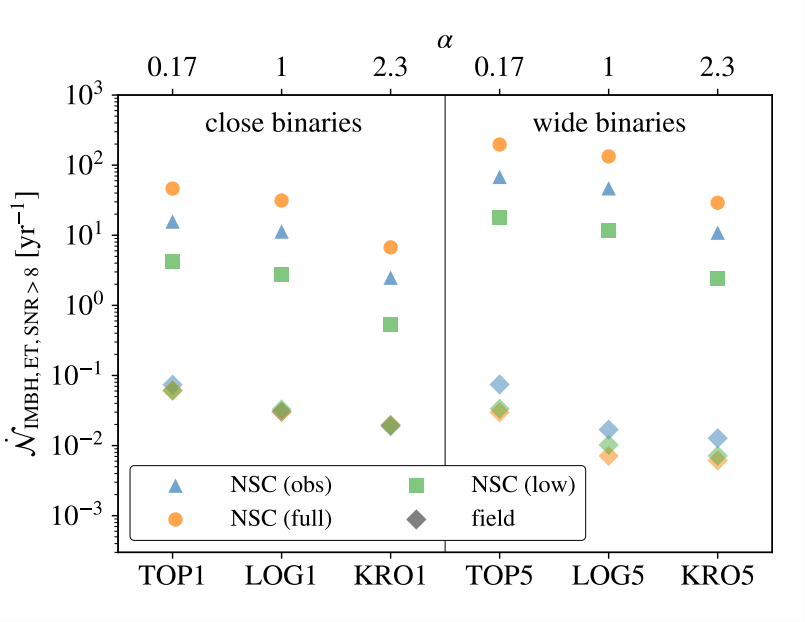

(IMBH mergers)

We use the ***python*** package GWTOOLBOX (Yi et al., 2022a,b) to calculate the detection probability of each merger.

Detection rates by LVK O4 (SNR>8)

- All mergers: $\dot{\mathcal{N}}_{\rm LVK,SNR>8} \sim 0.9 - 9.3\ {\rm yr}^{-1}$ in total,
  $\sim 0.5 - 9.1\ {\rm yr}^{-1}$ for NSC mergers, and $\sim 0.09 - 2.1\ {\rm yr}^{-1}$ for field mergers
- Intermediate-mass BH (IMBH) mergers ($m_1 > 100\ {\rm M}_\odot$):
  $\dot{\mathcal{N}}_{\rm LVK,IMBH,SNR>8} \sim 0.04 - 1.5\ {\rm yr}^{-1}$ in NSCs and $\lesssim 0.002\ {\rm yr}^{-1}$ in galaxy fields
- Fraction in NSCs:
  $\mathcal{F}_{\rm NSC} \sim 41 - 80\%$ for S12 (close binaries) and $\sim 92 - 98\%$ for SB13 (wide binaries)

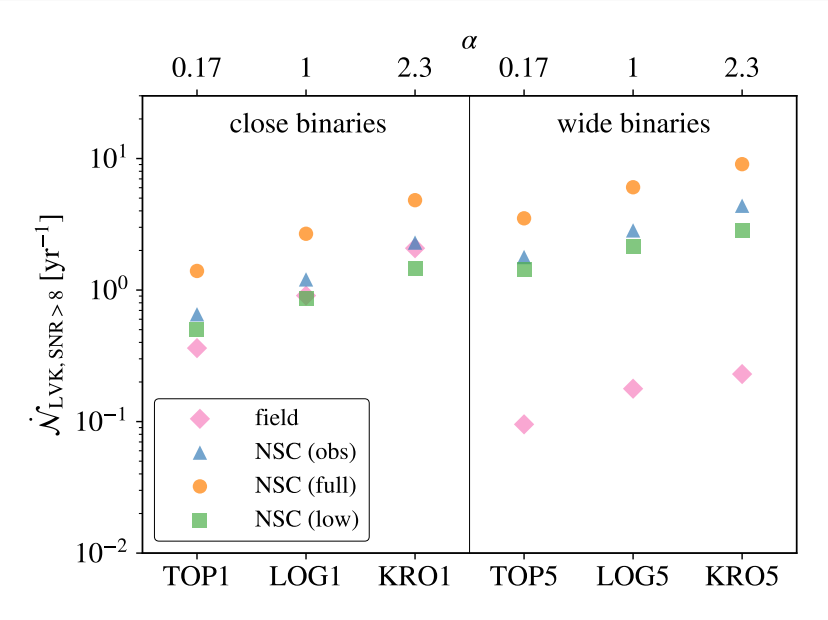

(all mergers)

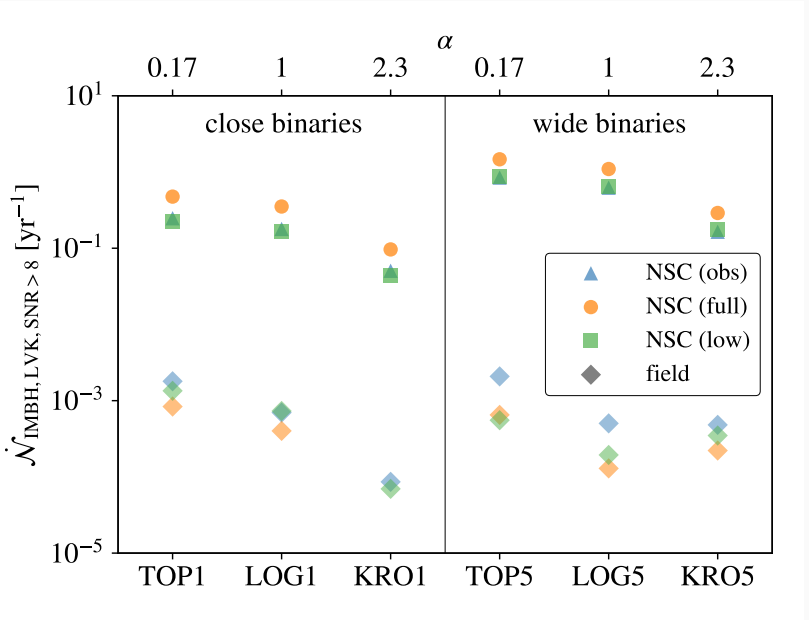

(IMBH mergers)

Our results are consistent with current observations of massive BBH mergers involving IMBHs and mass-gap BHs by LVK (Abbott et al., 2022a,b).

Summary

- The properties of Pop III binary stars are still unknown (likely dominated by wide binaries, different from present-day stars). → There are significant uncertainties in theoretical predictions on Pop III BBH mergers.
- An alternative channel based on dynamical hardening in nuclear star clusters (NSCs) can be as efficient as the classical isolated binary stellar evolution (IBSE) channel in producing Pop III BBH mergers at $z \lesssim 9$, which contributes $\sim 1 - 88\%$ of the detection rate of Pop III mergers by ET.
  Higher contributions from NSC mergers are achieved by initially wider binary stars, more top-heavy IMFs, and higher occupation fractions of NSCs.
- Only a small fraction $(4 - 12\%)$ of Pop III BBHs fall into NSCs, but a significant fraction $(\sim 45 - 64\%)$ of them merge at $z > 0$, including initially wide binaries.
- Pop III BBH mergers can contribute $\sim 2 - 32\%$ of the total SGWB inferred from observations (Abbott et al., 2023) at $\nu \lesssim 10$ Hz.
- Pop III BBH mergers in NSCs are more massive than those in galaxy fields from IBSE, so they dominate the Pop III SGWB below ~ 20 Hz in most cases.
  A significant fraction (up to 84%) of Pop III BBH mergers in NSCs involve at least one IMBH above 100 $\mathrm{M}_\odot$, while such mergers are extremely rare from IBSE.
- Most ($\gtrsim 90\%$) Pop III BBH mergers in our models are detectable by ET with a promising rate of $\dot{\mathcal{N}}_{\mathrm{ET,SNR>8}} \sim 50 - 1370\ \mathrm{yr}^{-1}$, including IMBH mergers with $\dot{\mathcal{N}}_{\mathrm{ET,IMBH,SNR>8}} \sim 0.5 - 200\ \mathrm{yr}^{-1}$.

BONUS SLIDES

Summary of runs

Run	α	$p(q)$	$p(\pi)$	$p(e)$	$f_{\rm occ}$	$M_{\star,\rm min}$ [$M_\odot$]	$\epsilon_{\rm BBH}$ [10^{-4} $M_\odot^{-1}$]	$\epsilon^{\rm GW}_{\rm all\ (field/NSC)}$ [10^{-5} $M_\odot^{-1}$]	$f_{\rm NSC}$	$f^{\rm GW}_{\rm field/NSC}$	$f_{\rm infall}$
LOG1_obs	1	S12	S12	S12	$\hat{f}_{\rm occ}$	10^6	4.78	6.49 (5.33/1.16)	17.9%	11.6%/62.8%	3.87%
TOP1_obs	0.17	S12	S12	S12	$\hat{f}_{\rm occ}$	10^6	2.58	2.38 (1.66/0.722)	30.3%	6.73%/64.1%	4.36%
KRO1_obs	2.3	S12	S12	S12	$\hat{f}_{\rm occ}$	10^6	7.05	11.8 (10.2/1.57)	13.3%	15.1%/60.6%	3.67%
LOG5_obs	1	SB13	SB13	$2e$	$\hat{f}_{\rm occ}$	10^6	10	3.64 (0.685/2.95)	81.2%	0.716%/61%	4.82%
TOP5_obs	0.17	SB13	SB13	$2e$	$\hat{f}_{\rm occ}$	10^6	7.94	2.76 (0.283/2.48)	89.8%	0.376%/62.5%	4.99%
KRO5_obs	2.3	SB13	SB13	$2e$	$\hat{f}_{\rm occ}$	10^6	8.9	3.14 (0.755/2.38)	75.9%	0.888%/58.6%	4.56%
LOG1_full	1	S12	S12	S12	1	10^6	4.78	7.98 (5.27/2.71)	34%	12.2%/58.9%	9.65%
TOP1_full	0.17	S12	S12	S12	1	10^6	2.57	3.32 (1.63/1.69)	50.8%	7.13%/60.3%	10.9%
KRO1_full	2.3	S12	S12	S12	1	10^6	7.05	13.7 (10.1/3.64)	26.5%	15.7%/56.4%	9.14%
LOG5_full	1	SB13	SB13	$2e$	1	10^6	10	7.29 (0.674/6.62)	90.8%	0.761%/55.6%	11.9%
TOP5_full	0.17	SB13	SB13	$2e$	1	10^6	7.9	5.85 (0.273/5.57)	95.3%	0.394%/56.8%	12.4%
KRO5_full	2.3	SB13	SB13	$2e$	1	10^6	8.9	6.01 (0.741/5.27)	87.7%	0.937%/52.9%	11.2%
LOG1_low	1	S12	S12	S12	$\hat{f}_{\rm occ}$	10^{10}	4.78	6.07 (5.34/0.73)	12%	11.5%/50.2%	3.04%
TOP1_low	0.17	S12	S12	S12	$\hat{f}_{\rm occ}$	10^{10}	2.57	2.17 (1.65/0.513)	23.7%	6.68%/55.2%	3.62%
KRO1_low	2.3	S12	S12	S12	$\hat{f}_{\rm occ}$	10^{10}	7.05	11.2 (10.3/0.894)	8%	15%/45.8%	2.77%
LOG5_low	1	SB13	SB13	$2e$	$\hat{f}_{\rm occ}$	10^{10}	10	2.71 (0.686/2.02)	74.7%	0.711%/51.9%	3.89%
TOP5_low	0.17	SB13	SB13	$2e$	$\hat{f}_{\rm occ}$	10^{10}	7.9	2.16 (0.277/1.89)	87.2%	0.366%/56.5%	4.22%
KRO5_low	2.3	SB13	SB13	$2e$	$\hat{f}_{\rm occ}$	10^{10}	8.9	2.18 (0.755/1.42)	65.4%	0.879%/45.4%	3.52%

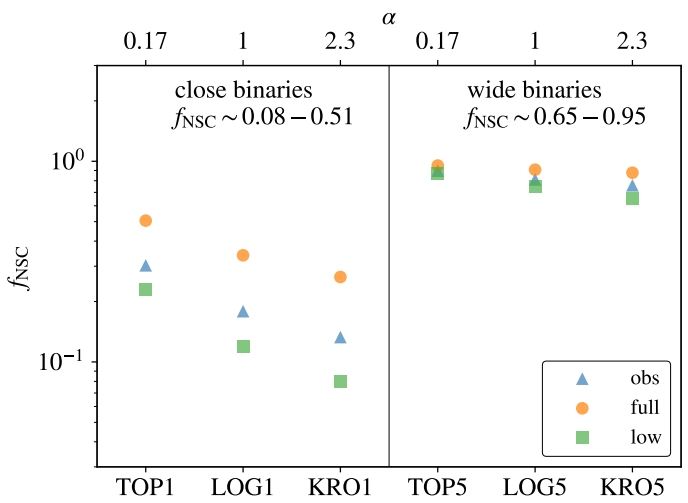

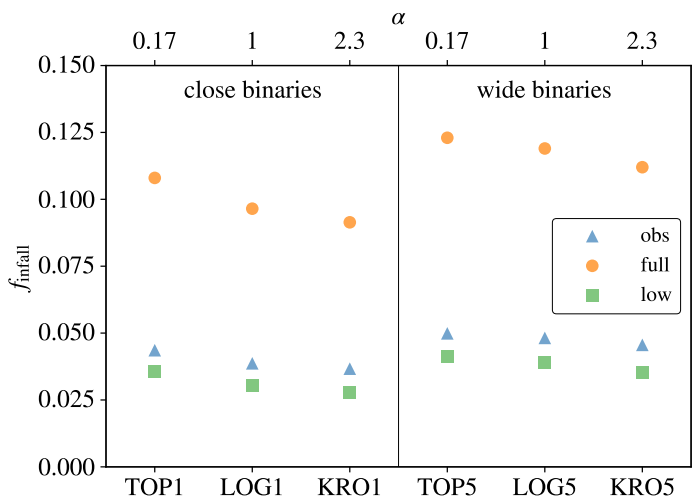

(A) IMF (OBS): S12 vs. SB13

S12 (close binaries)

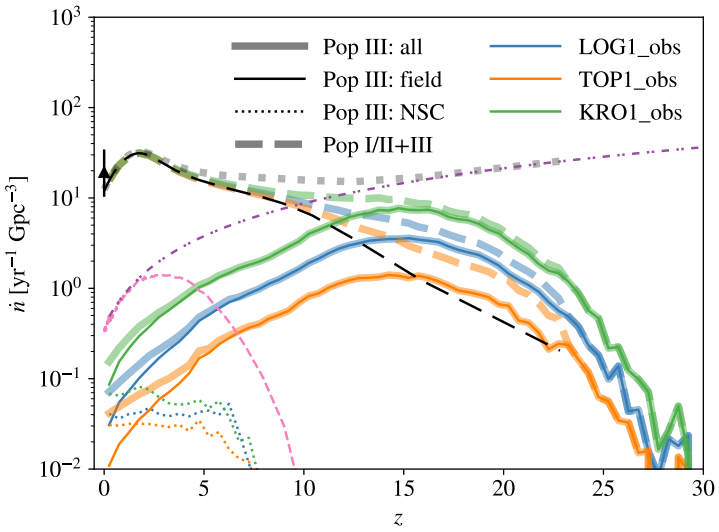

SB13 (wide binaries)

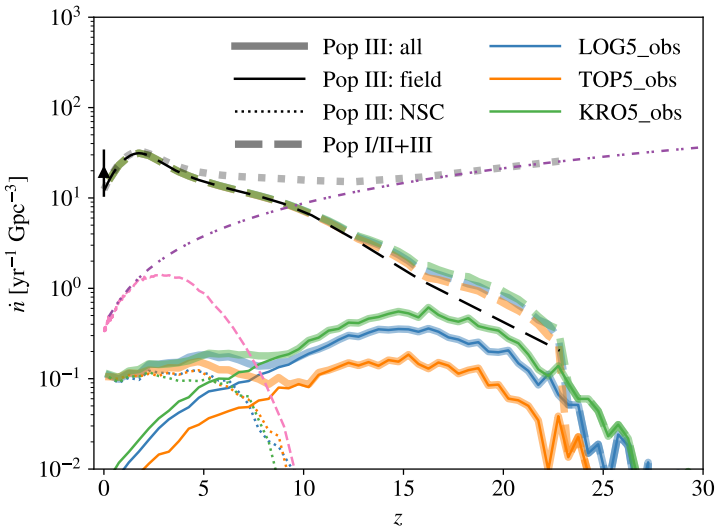

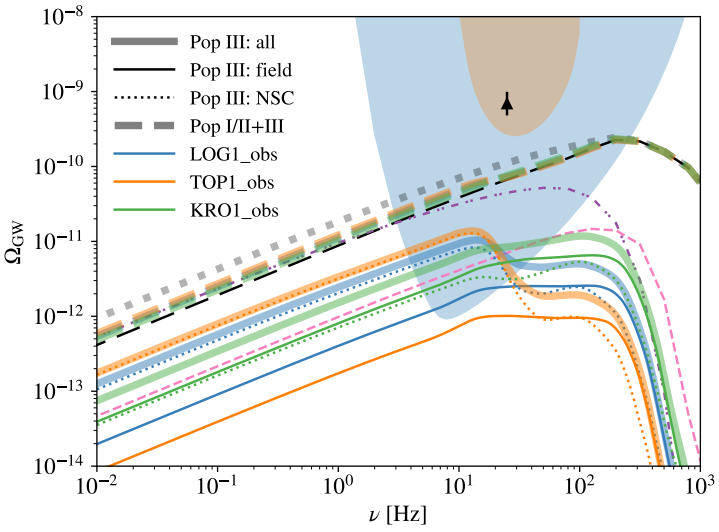

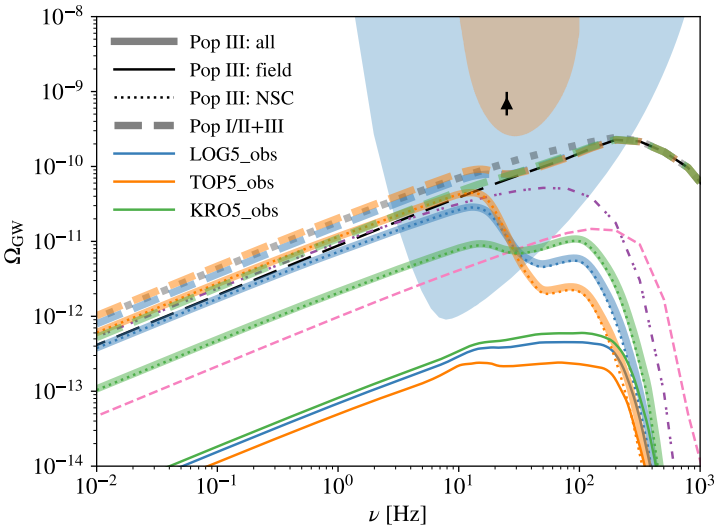

(b) IBS (obs): top-heavy vs. bottom-heavy

TOP (top-heavy)

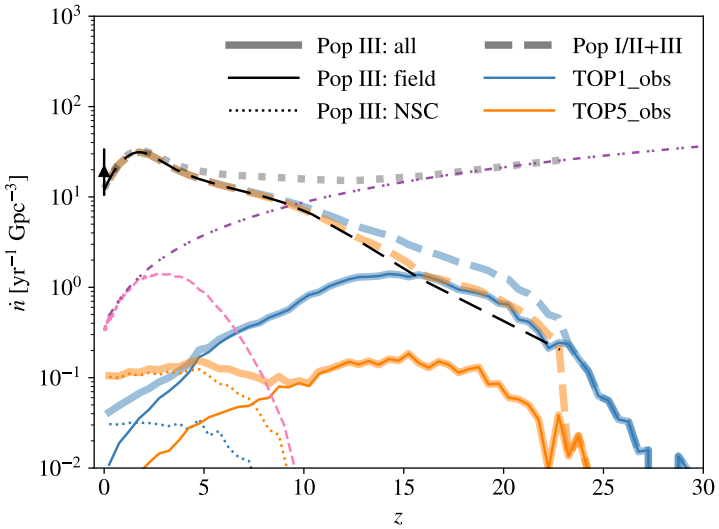

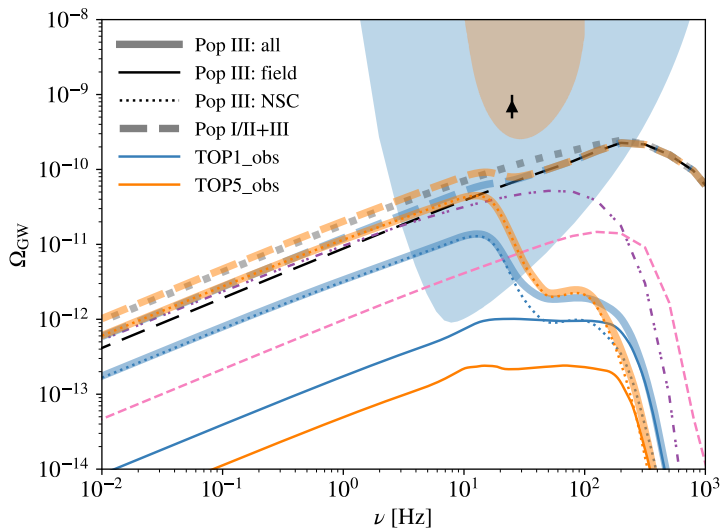

KRO (bottom-heavy)

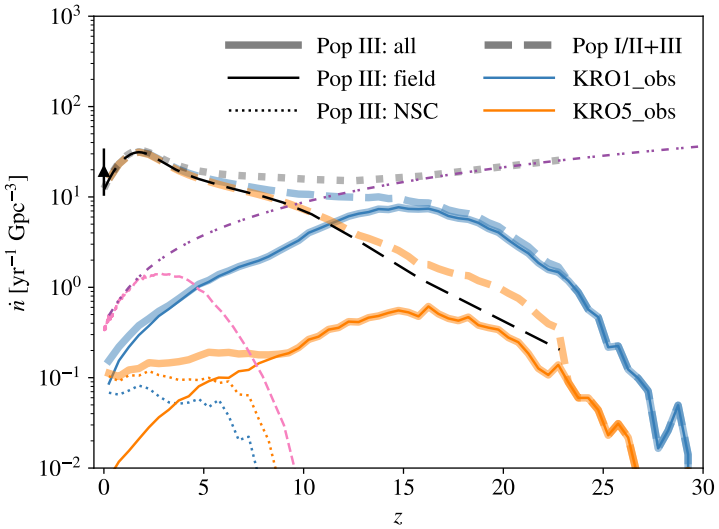

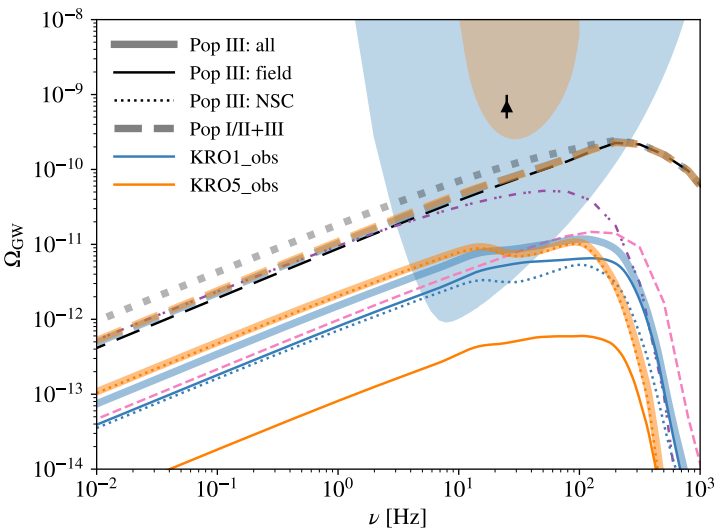

(c) NSC occupation (log-flat): S12 vs. SB13

S12 (close binaries)

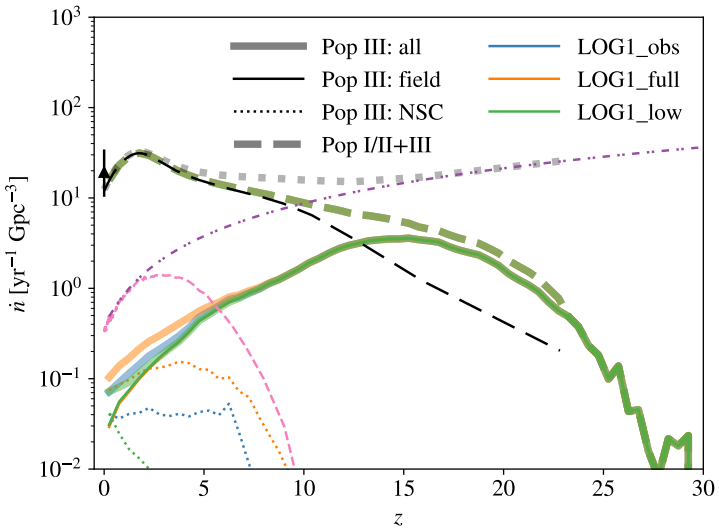

SB13 (wide binaries)

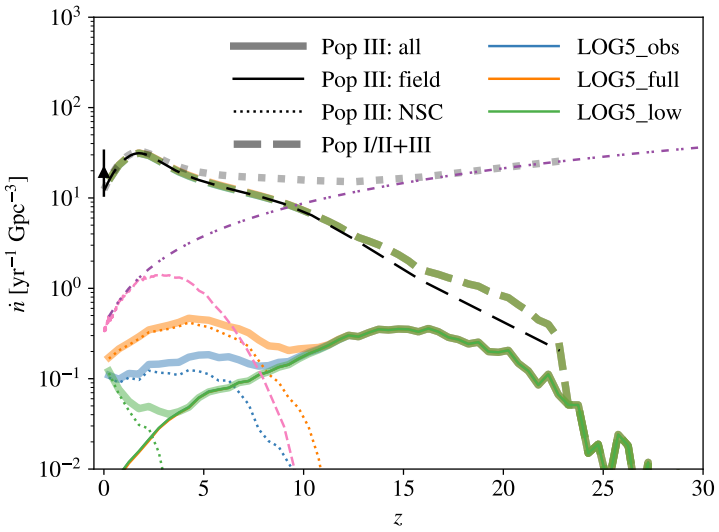

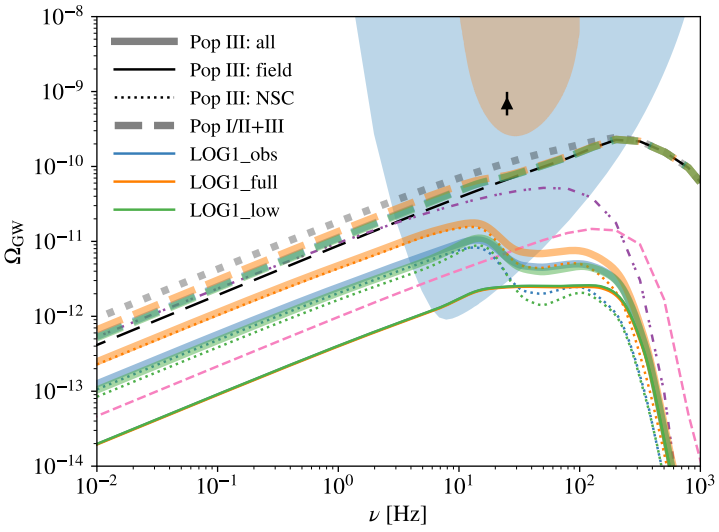

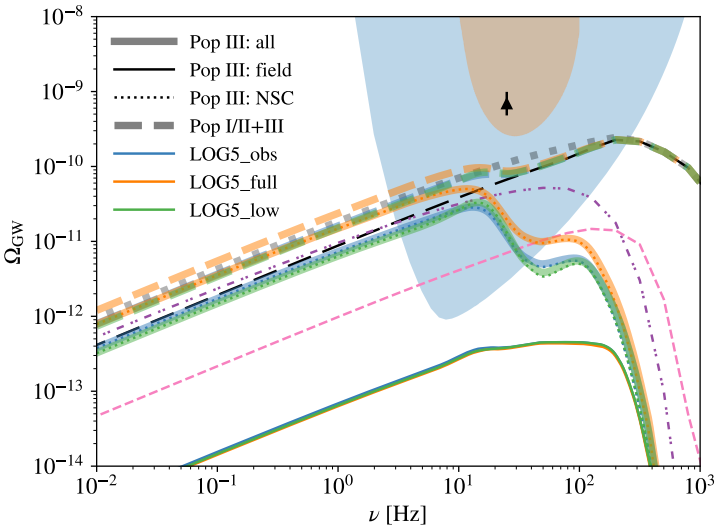

Star formation rate density (SFRD)

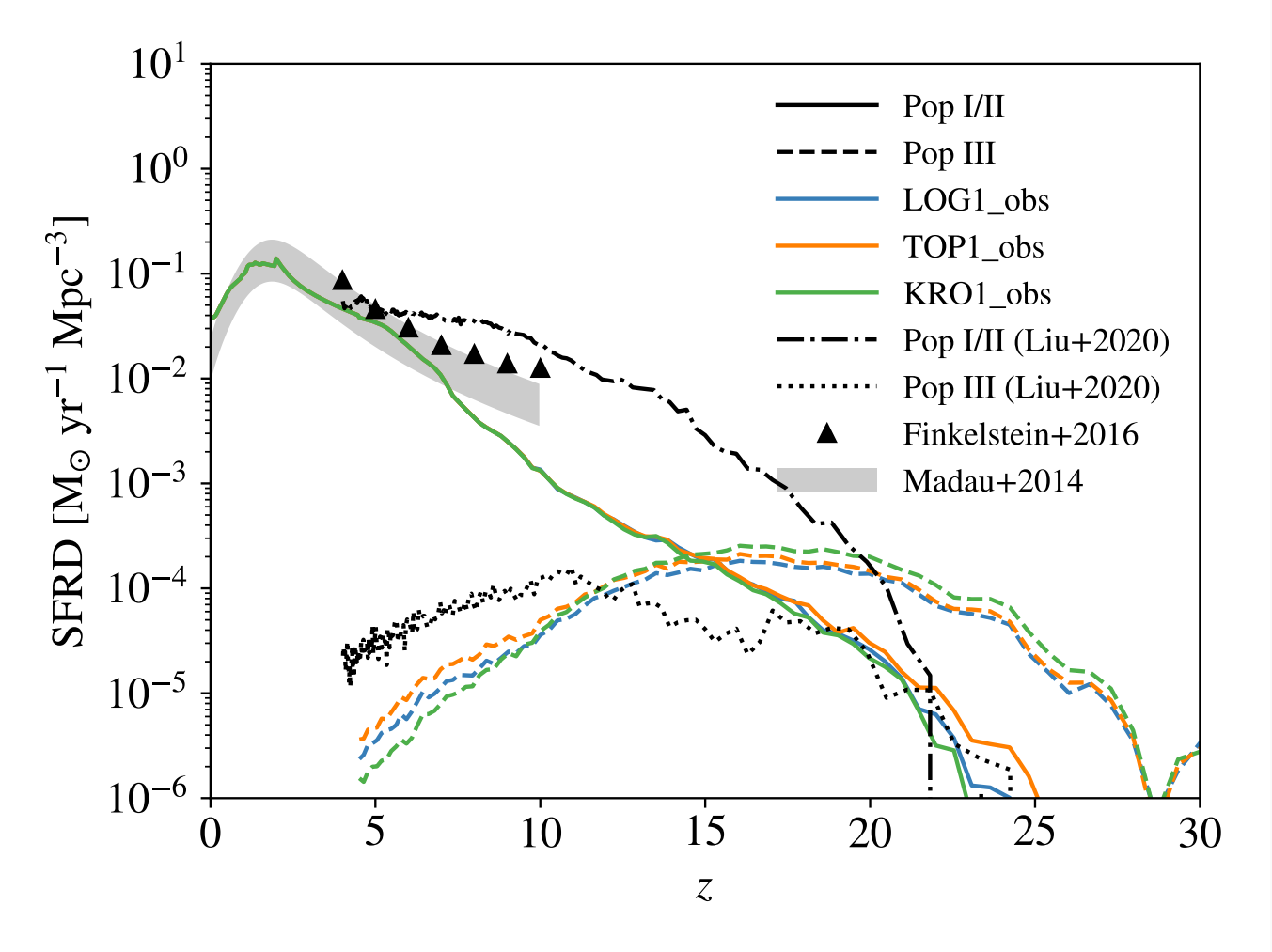

The shaded region and data points show observational results from Madau & Dickinson (2014) and Finkelstein (2016), respectively. The dotted and dash-dotted curves show the predictions for Pop III and Pop I/II mergers from the cosmological simulation in Liu & Bromm (2020a,b).

Host systems of Pop III BBH mergers (LOG1_obs)

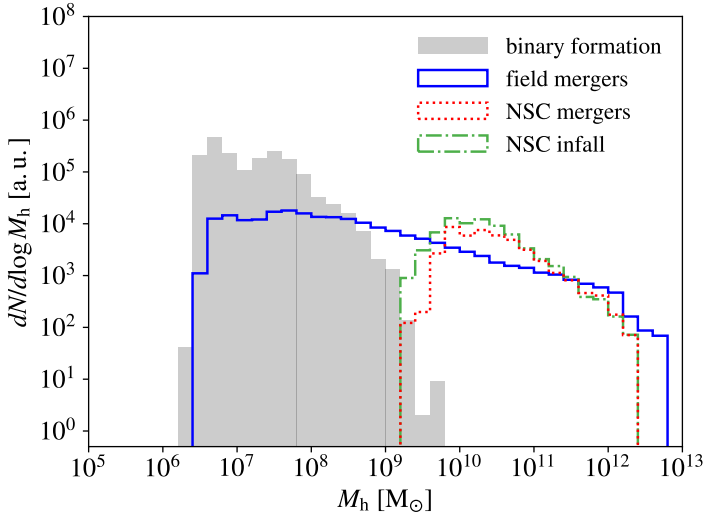

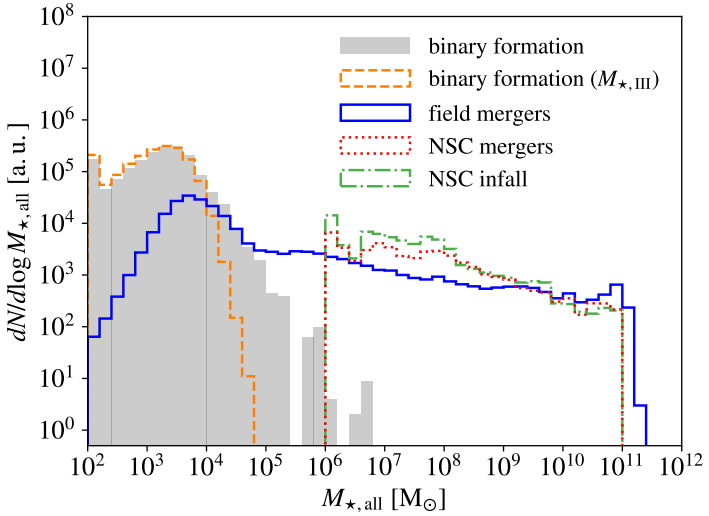

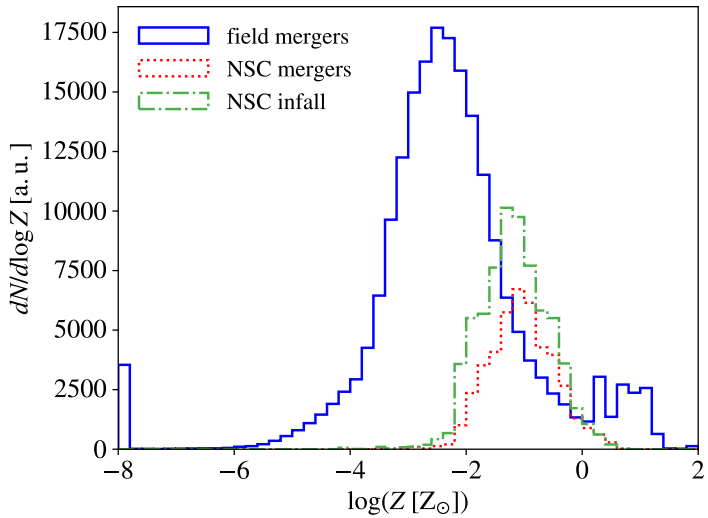

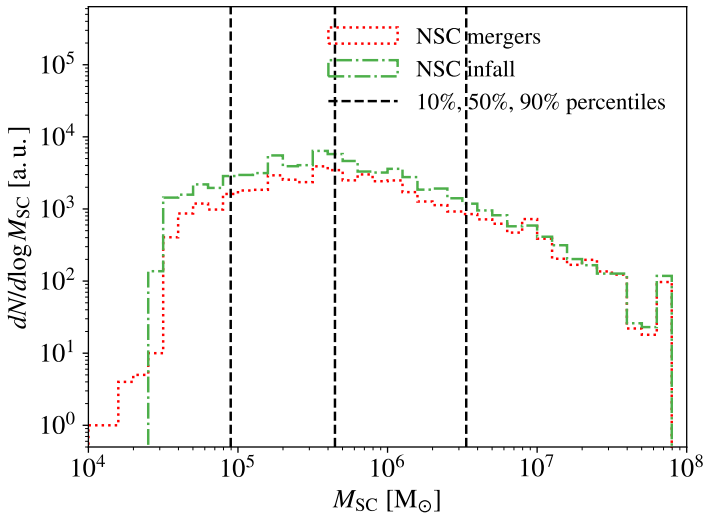

Meger rate per galaxy (LOG1_obs)

stellar mass function

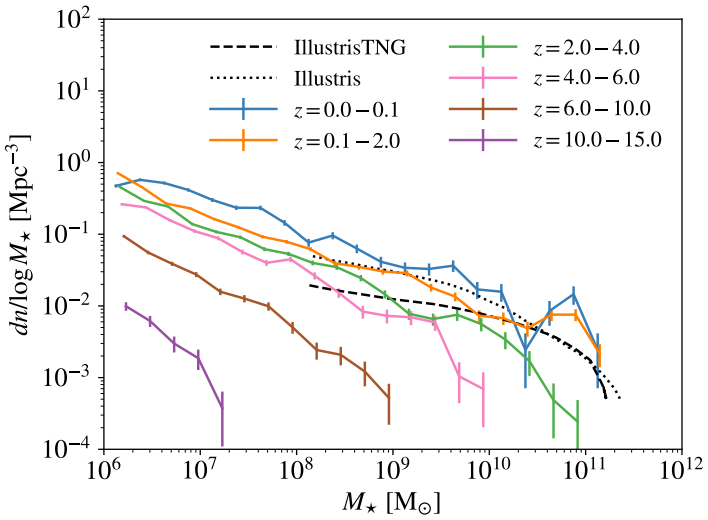

all mergers

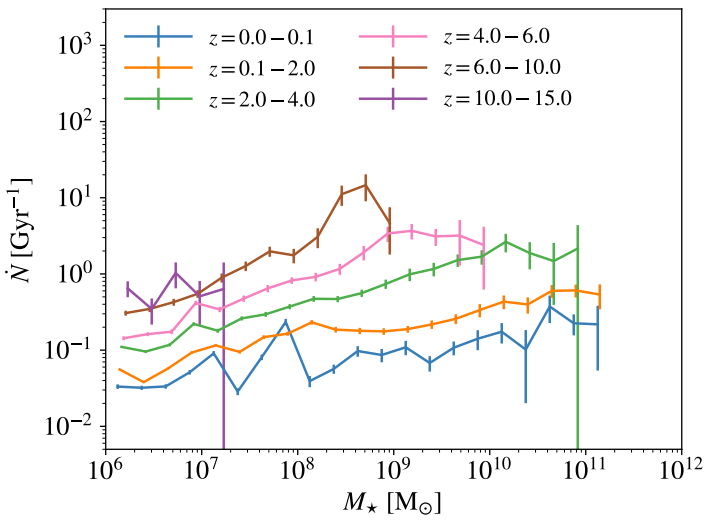

field mergers

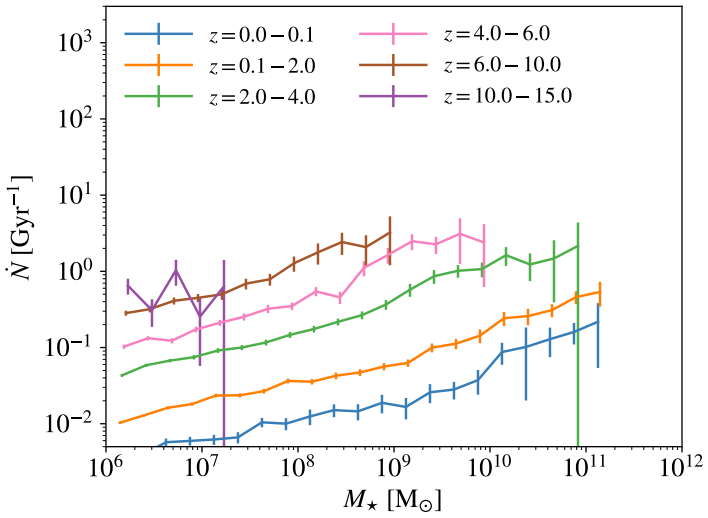

NSC mergers

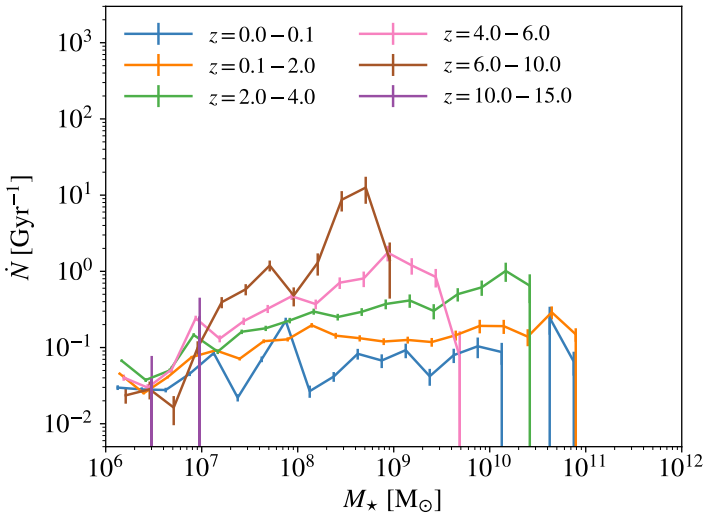

The results from Illustris and IllustrisTNG simulations are taken from Pillepich et al. (2018).

The special event GW190521

Unusual BH masses: $m_1 = 85^{+21}_{-14}\ \mathrm{M}_\odot$ and $m_2 = 66^{+17}_{-18}\ \mathrm{M}_\odot$

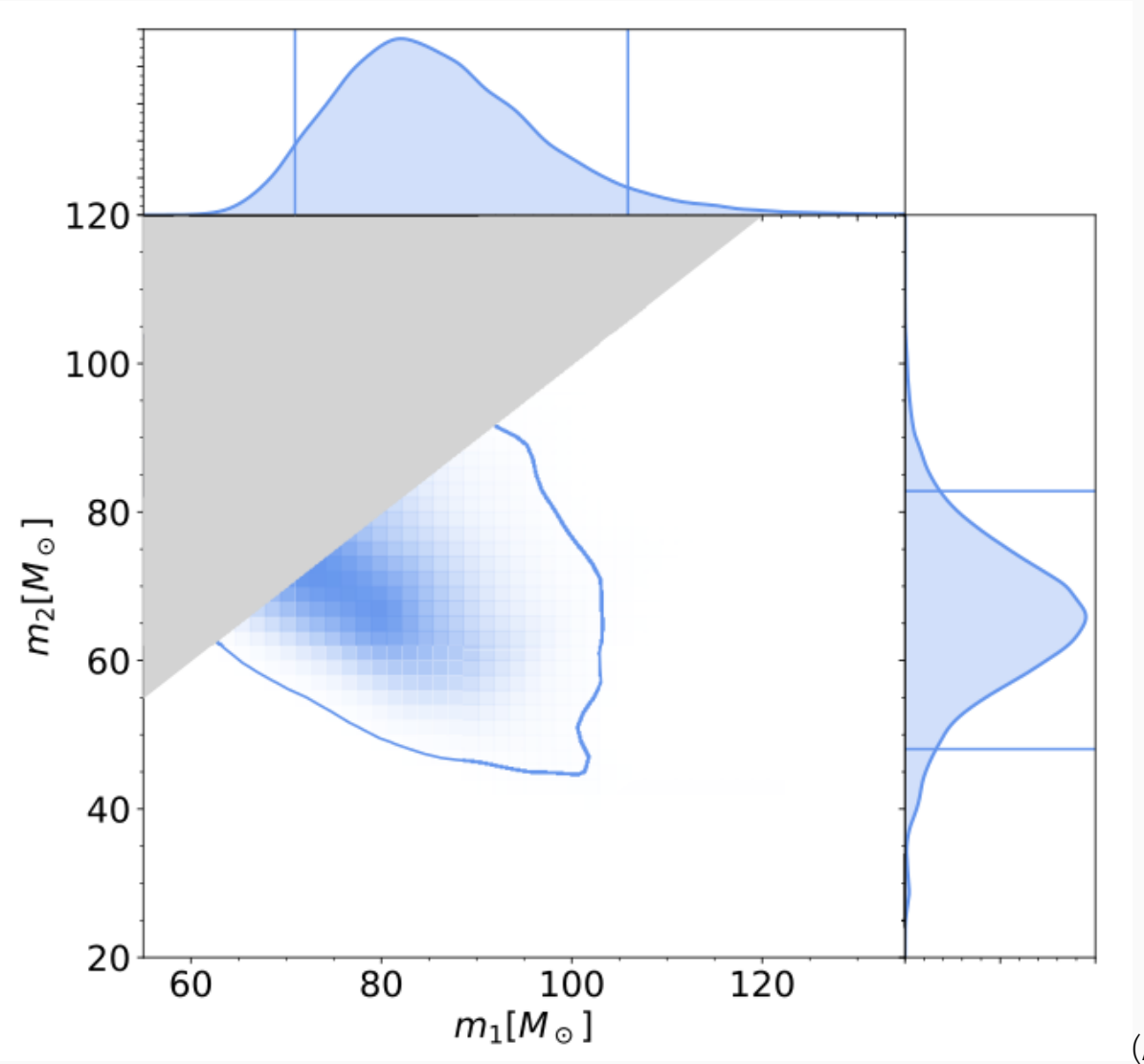

(Abbott et al., 2020)

Mass gap of pair-instability supernovae

Standard pair-instability mass gap: $\sim 50 - 130\ \mathrm{M}_\odot$

(see e.g., Heger et al. 2003; Belczynski et al. 2016; Woosley 2017; Marchant et al. 2019)

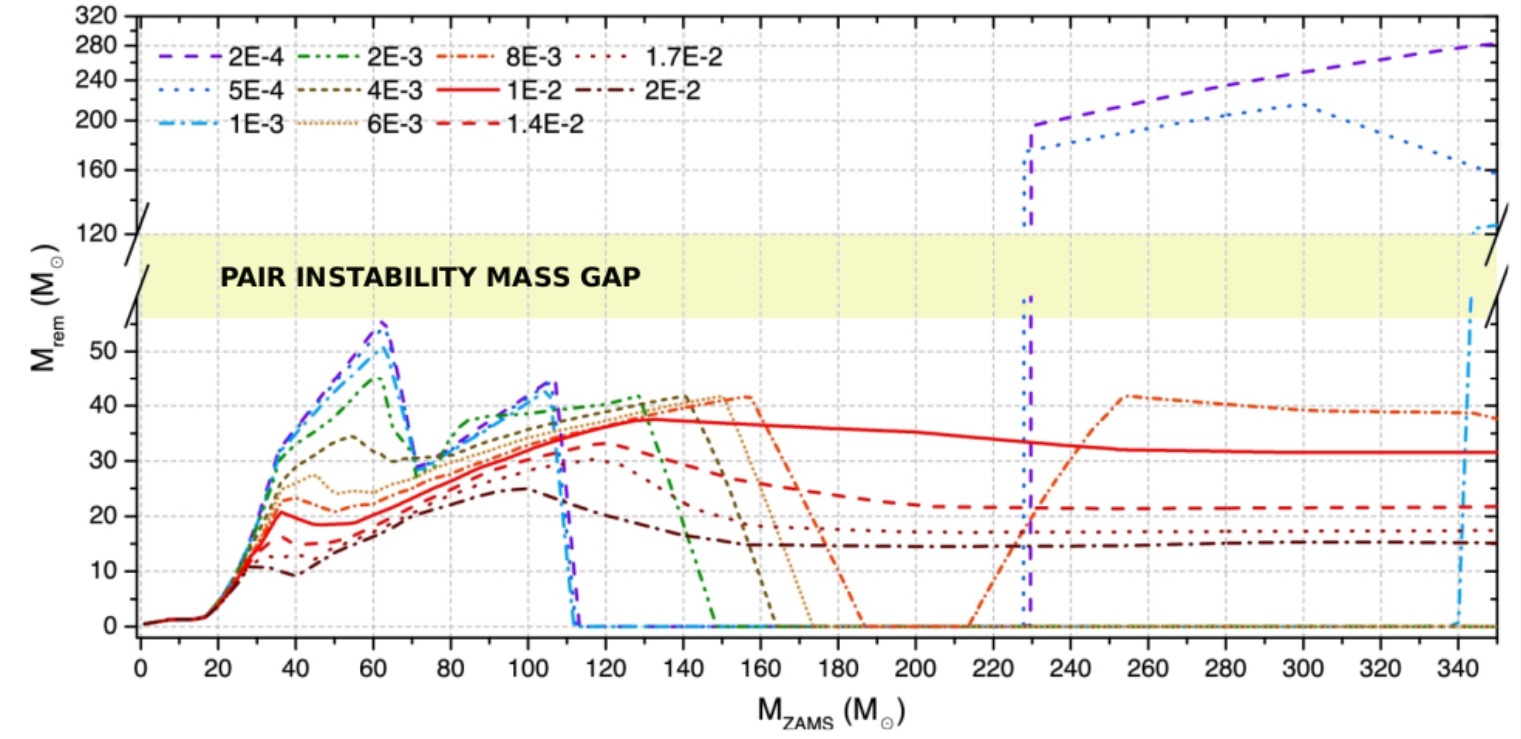

(Mapelli, 2020)

Pop III stars can retain most of their envelopes and form BHs up to $\sim 100\ \mathrm{M}_\odot$ before entering the pair-instability regime

(see, e.g., Farrell et al., 2021; Tanikawa et al., 2021a).

Mass-gap BHs via IBSE?

It is possible to form mass-gap BHs in wide binaries with weak interactions. **However, strongly interacting binaries that lead to BBH mergers in the IBSE channel hardly produce mass-gap BHs due to strong mass loss during binary interactions.**

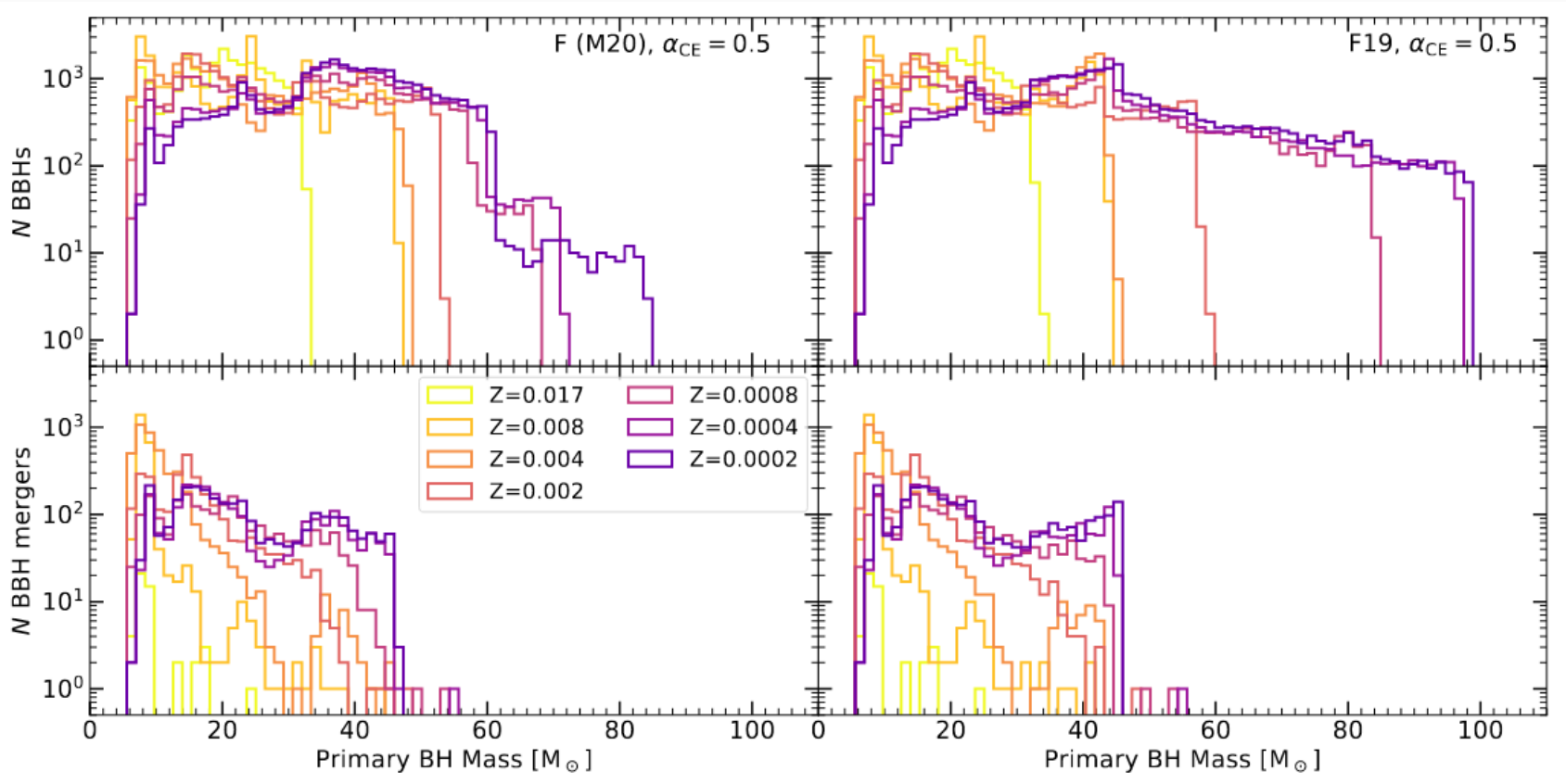

Mass distribution of primary BHs for all BBHs (top) and BBH mergers (bottom) predicted by SEVN (Iorio et al., 2023) for two pair-instability supernova models: M20 (Mapelli et al., 2020, left), F19 (Farmer et al., 2019, right)

MRD of massive BBHs via IBSE

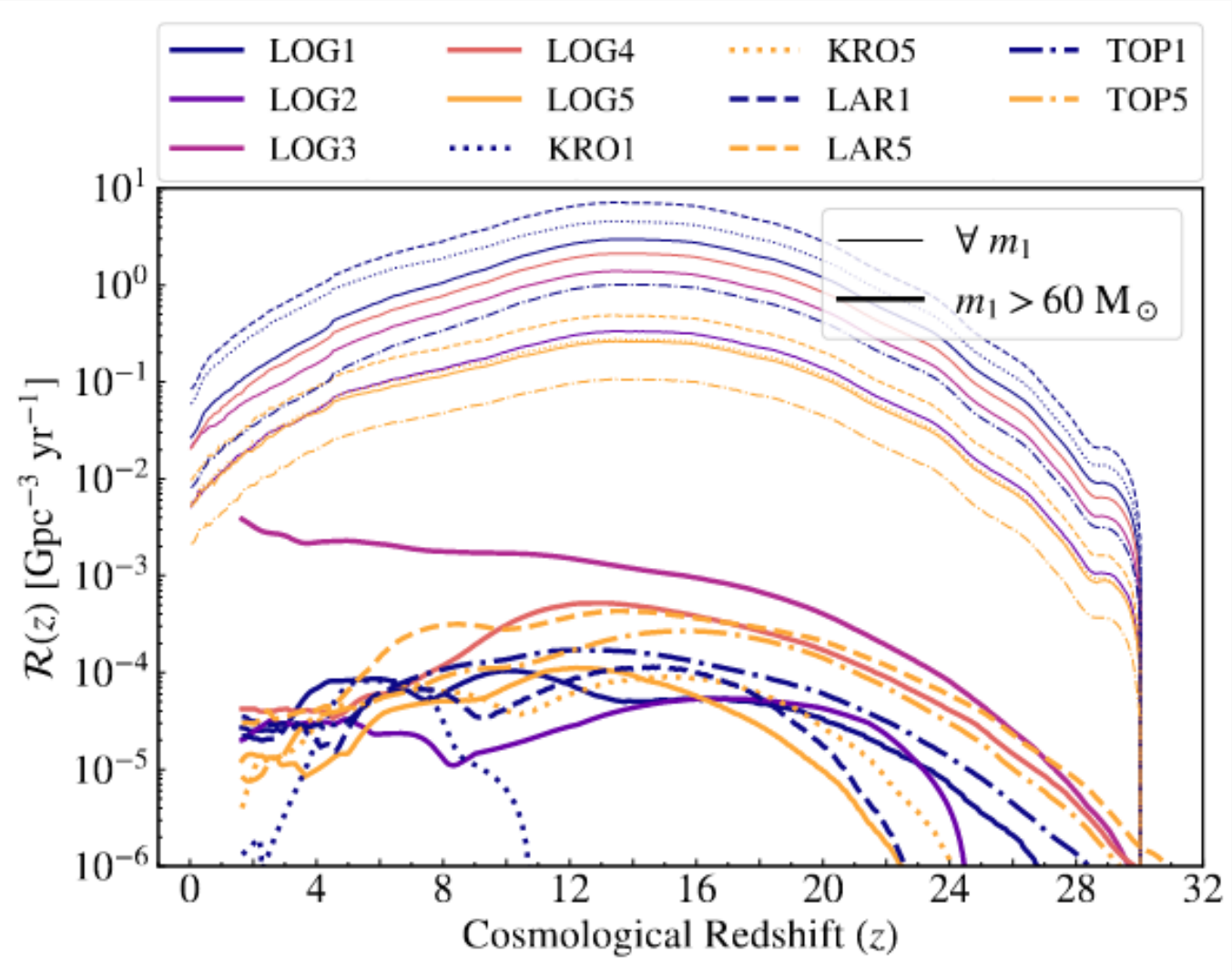

Evolution of merger rate density for all Pop III BBHs (thin) and those with primary BH masses above 60 $\mathrm{M}_\odot$ (thick) predicted by Santoliquido et al. (2023) for different initial conditions (shown with different colors, see their table 1).

MRD of massive BBHs via NSC-DH

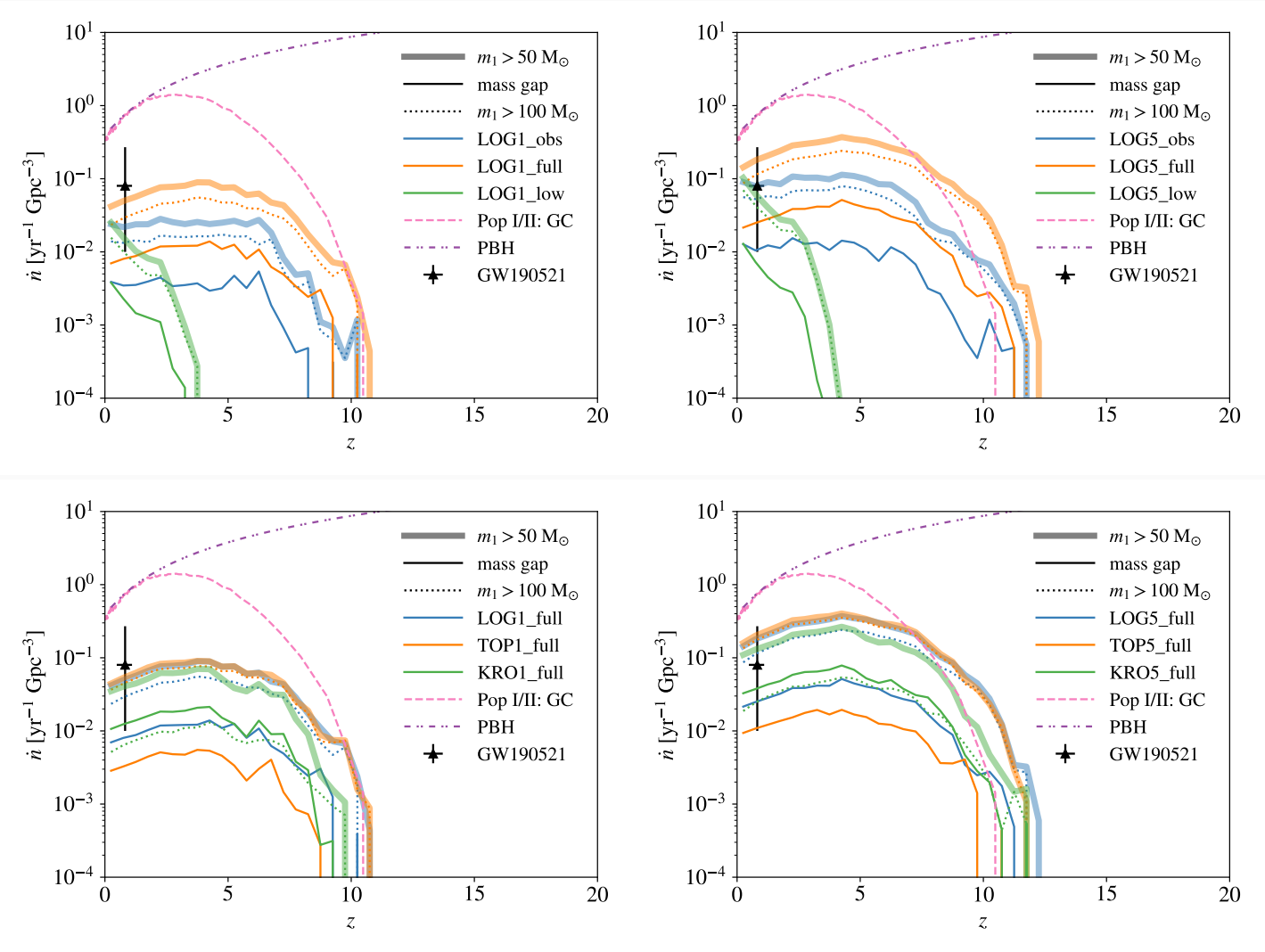

Mass-gap mergers: $m_1, m_2 \in [50, 130]\ \mathrm{M}_\odot$. Predicted: $\dot{n}_{\mathrm{gap}} \sim 0.0013 - 0.034\ \mathrm{yr}^{-1}\ \mathrm{Gpc}^{-3}$. Data point: merger rate density of GW190521-like objects inferred from observations (90% confidence interval): $\dot{n}_{\mathrm{gap,obs}}(z \sim 1) = 0.08^{+0.19}_{-0.07}\ \mathrm{yr}^{-1}\ \mathrm{Gpc}^{-3}$ (Abbott et al., 2022a)

Tracking Pop III BBHs in a-sloth

- Pop III star-forming halo $\rightarrow$ mass of Pop III stars formed $\delta M_{\star,\mathrm{III}}$ + binary mass fraction $f_{\mathrm{B}} \sim 0.7$ (Liu et al., 2021) + Mass fraction of binaries that become BBHs f_{BBH} and average mass of progenitors of BBHs $\bar{m}_{\mathrm{p,BBH}}$ from BPS (Costa et al., 2023)+boost factor $f_{\mathrm{boost}} = 50$ for better statistics $\rightarrow$ expected number of BBHs $\lambda_{\mathrm{BBH}} = f_{\mathrm{boost}} f_{\mathrm{B}} f_{\mathrm{BBH}} \delta M_{\star,\mathrm{III}} / \bar{m}_{\mathrm{p,BBH}}$
- Draw the number of BBHs N_{BBH} to sample in this timestep from a Poisson distribution with parameter λ_{BBH}
- If $N_{\mathrm{BBH}} > 0$, draw N_{BBH} BBHs randomly from the input BPS catalog generated by SEVN (Costa et al., 2023)
- Distribute BBHs in haloes during initial formation and halo mergers, based on the spatial distribution of Pop III remnants from cosmological simulations (Liu & Bromm, 2020a,b)

Initial distribution of Pop III remnants

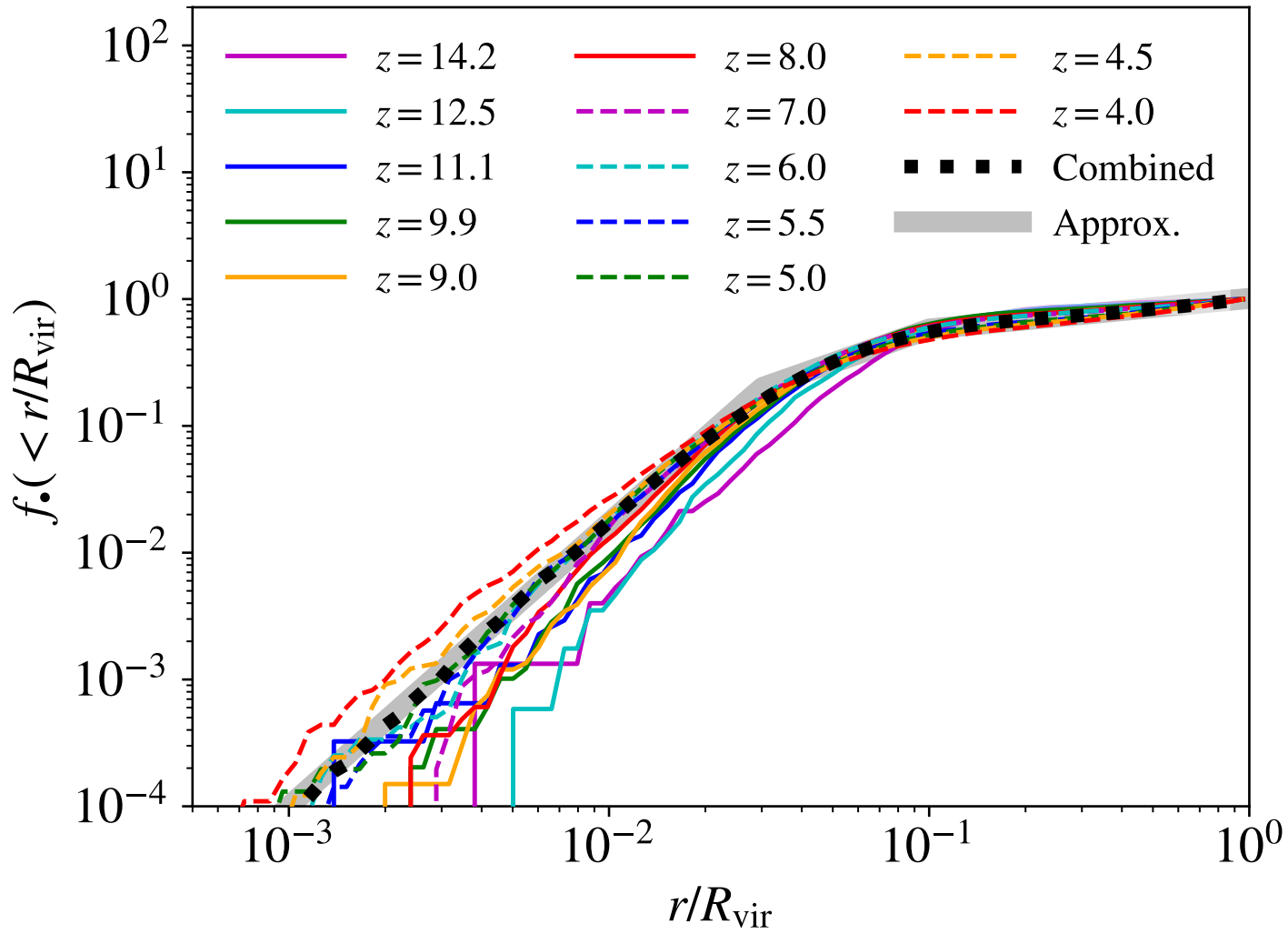

In-fall of Pop III remnants towards NSCs

$dr/dt \simeq -r/\tau_{\rm DF}$

Dynamical friction timescale: $\tau_{\rm DF} \equiv \tau_{\rm DF}(r|e_{\rm if}, m_\bullet, M_\star, R_\star, \gamma_\star)$

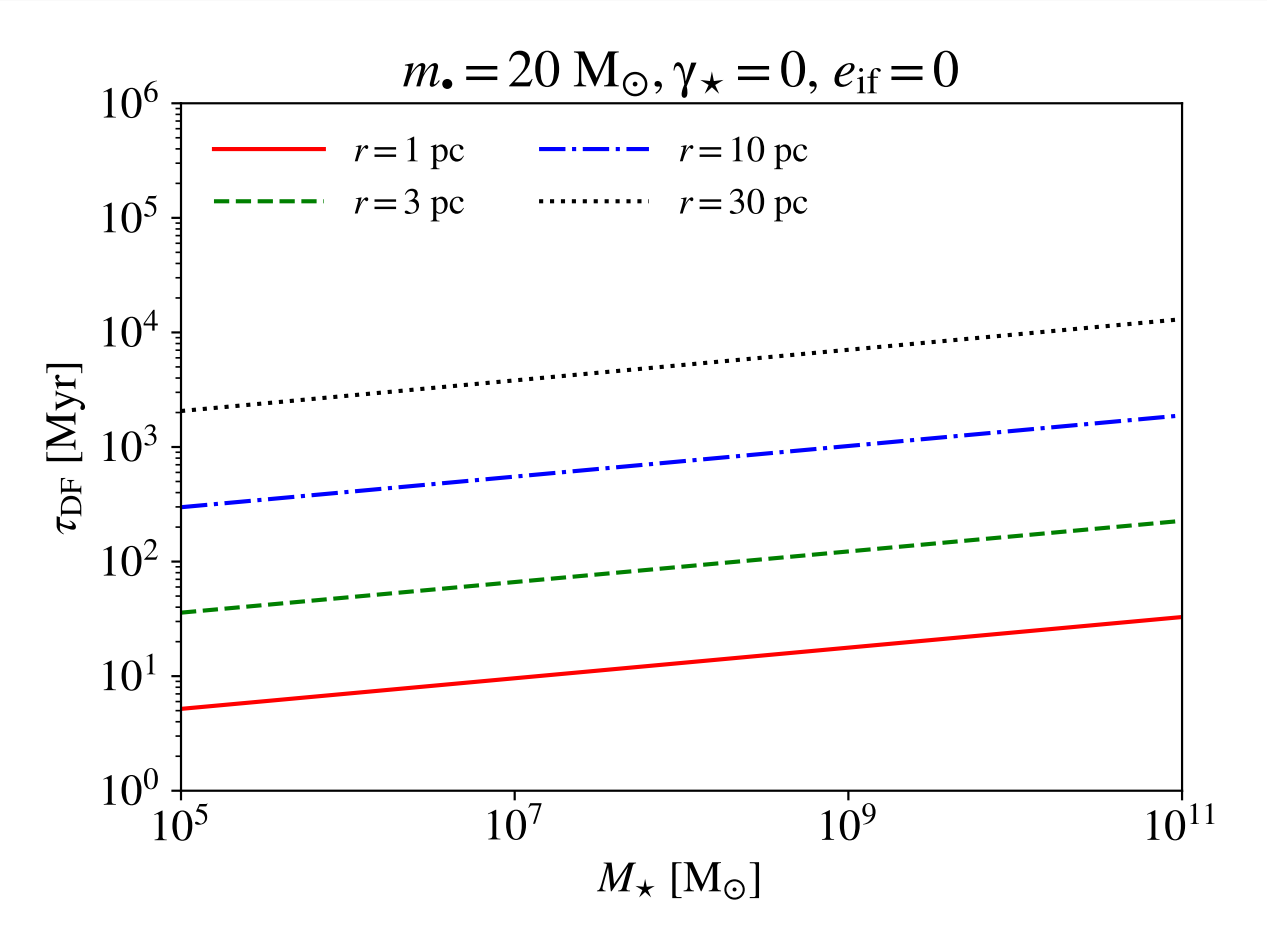

(based on the $\tau_{\rm DF}$ formula from Arca-Sedda 2016)

Evolution of Pop III remnant binaries in NSCs

Hard binaries sink into cluster cores by dynamical friction where DH and GW emission drive them to mergers.

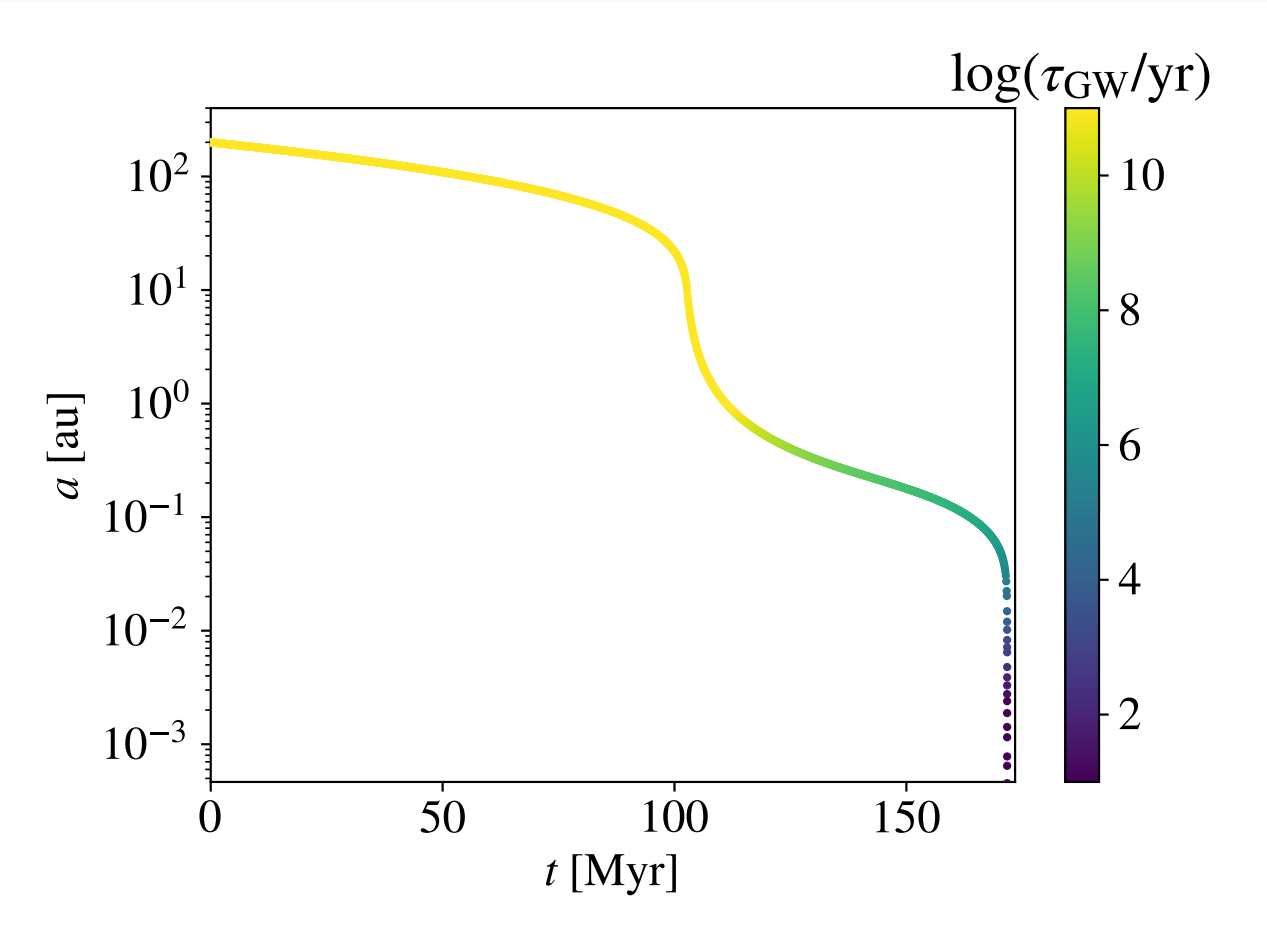

(for a massive GW190521-like BH-BH binary ($m_1 = 85\ \mathrm{M}_\odot$, $m_2 = 66\ \mathrm{M}_\odot$, $a_0 = 200\ \mathrm{au}$, $e_0 = 0$) in a Milky Way-like NSC ($M_{\mathrm{SC}} = 2.5 \times 10^7\ \mathrm{M}_\odot$, $R_{\mathrm{SC}} = 4.4\ \mathrm{pc}$, $\gamma_{\mathrm{SC}} = 1.8$) with a core density $\rho_\star \sim 2.5 \times 10^7\ \mathrm{M}_\odot\ \mathrm{pc}^{-3}$)

Galaxy & NSC models: empirical scaling relations

Galaxy mass $M_\star \rightarrow$ galaxy size $R_\star$, NSC mass $M_{\rm SC} \rightarrow$ NSC size $R_{\rm SC}$
Compactness parameters ($\gamma_\star$ and $\gamma_{\rm SC}$): drawn randomly

- Galaxy size-mass relation (Arca-Sedda & Capuzzo-Dolcetta, 2014; Somerville et al., 2018)

$$R_\star = [2^{1/(3-\gamma_\star)}-1]\,\max[0.02R_{\rm vir}, 2.37(M_\star/10^{11}\,{\rm M}_\odot)^{0.14}\,{\rm kpc}]\,,\ \gamma_\star \sim 0-2$$

- NSC-galaxy mass relation (Neumayer et al., 2020)

$$\log(M_{\rm SC}/{\rm M}_\odot) = 0.48\log[M_\star/(10^9\,{\rm M}_\odot)] + 6.51$$

- NSC size-mass relation ($M_{\rm crit} \sim 2\times10^6\,{\rm M}_\odot$)

$$\log\left(\frac{R_{\rm eff}}{\rm pc}\right) \simeq \begin{cases} 0.54\,, & M_{\rm SC} < M_{\rm crit}\,, \\ 0.34\log\left(\frac{M_{\rm SC}}{{\rm M}_\odot}\right) - 1.59\,, & M_{\rm SC} \geq M_{\rm crit}\,, \end{cases}$$

$$R_{\rm SC} = (4/3)R_{\rm eff}\left[2^{1/(3-\gamma_{\rm SC})} - 1\right]\,, \quad \gamma_{\rm SC} \sim 0.65 - 2.55$$

Stellar-halo mass relation (for $z < 4.5$)

Halo mass $M_{\rm h} \rightarrow$ galaxy (stellar) mass $M_\star \rightarrow R_\star$, $M_{\rm SC}$, $R_{\rm SC}$

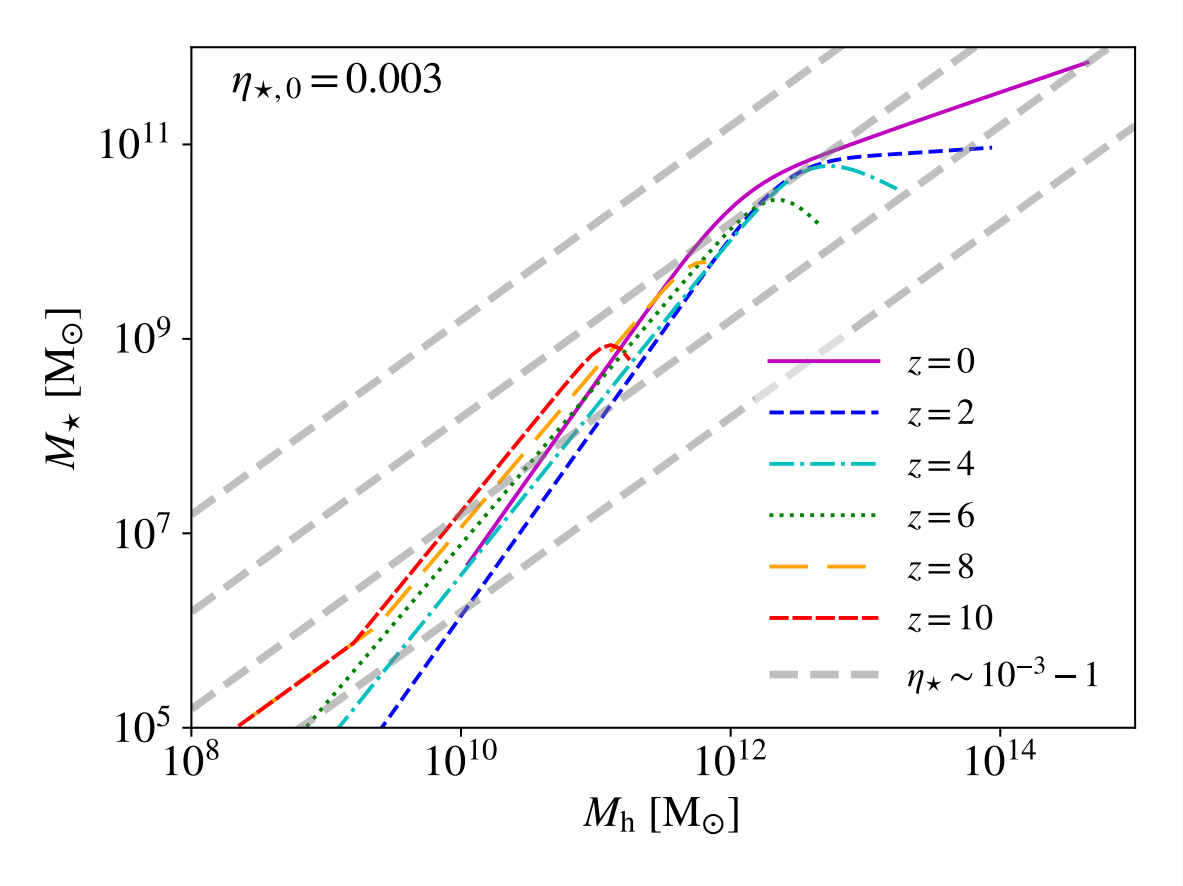

The merger trees from the cosmological simulation in Ishiyama et al. (2016) only cover $z \gtrsim 4.5$. The subsequent evolution of galaxies is followed with a simple model based on the stellar-halo mass relation from Behroozi et al. (2019).

Expansion of a Pop III binary (Sugimura et al., 2020)

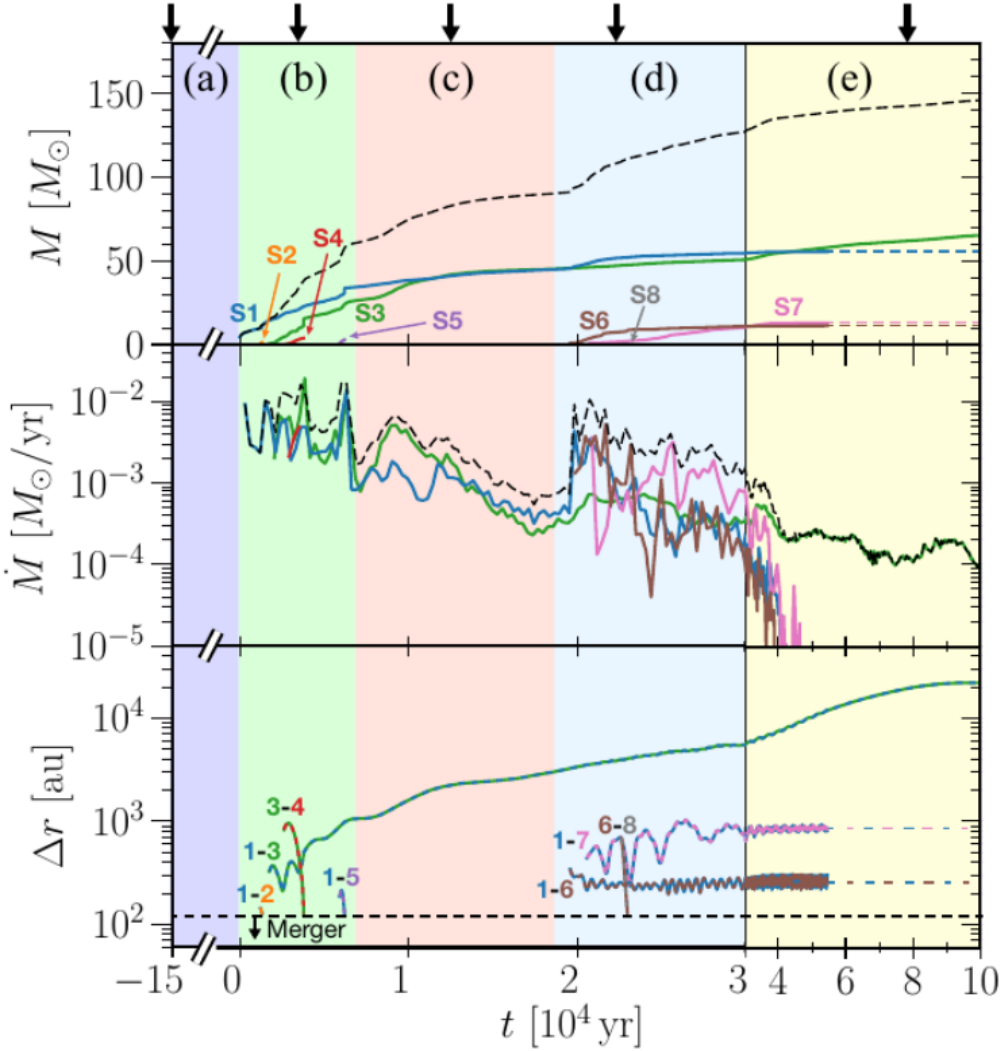

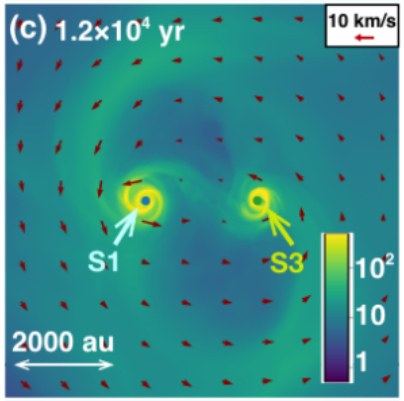

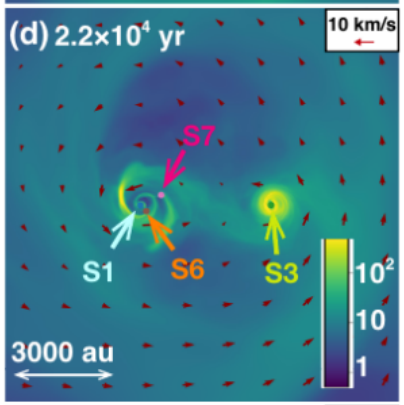

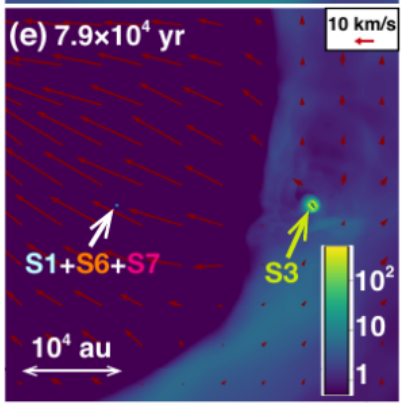

(see also Sugimura et al., 2023; Park et al., 2023, 2024)

Binary statistics of Pop III stars (Liu et al., 2021)

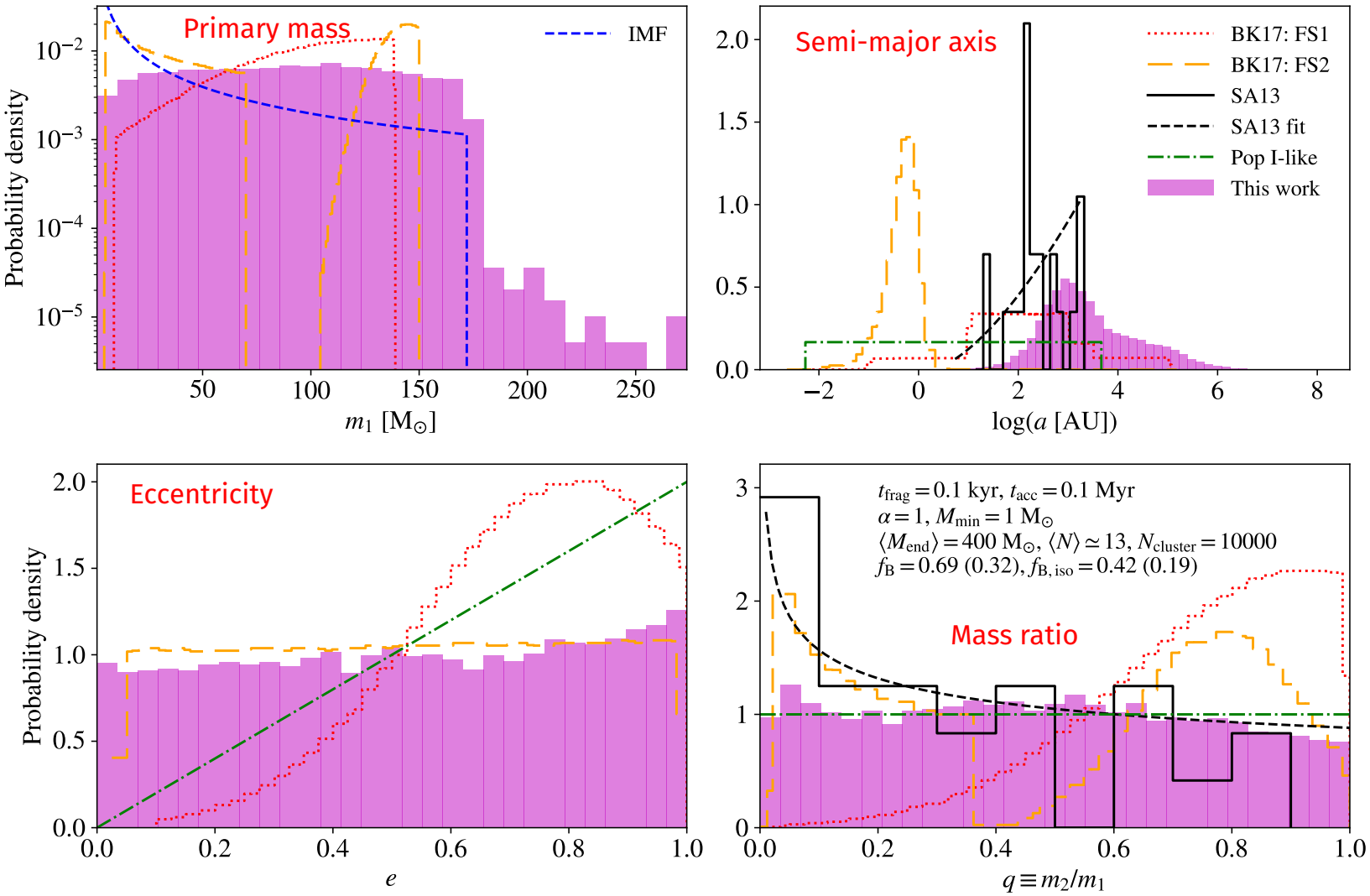

SA13 (protostars of a few $\mathrm{M}_\odot$): Stacy et al. (2013), BKI7 (mass enhanced protostar systems, Belczynski et al., 2017): FS1: $R_0 \sim 2000$ AU, based on Stacy et al. (2013), FS2: $R_0 \sim 7$ AU, based on Greif et al. (2012) (corrected version of fig. 9 in Liu et al., 2021, see also Liu et al., 2023b)

Outlook: better models for Pop III binaries

- Improvement of (radiative) magneto-hydrodynamic (MHD) simulations of Pop III star formation to better understand the evolution from protostars to (dry) star clusters
- Systematic investigations of the conditions of Pop III star formation (as extensions of, e.g., Hirano et al., 2014, 2015, 2018, 2023; Li et al., 2021) for complete statistics of Pop III star clusters
- Generative models for the initial conditions of star clusters based on simulations of star-forming clouds (e.g., Torniamenti et al., 2022)
- Multi-physics simulations of early star cluster formation and evolution, which couple (radiative) MHD, N-body dynamics as well as (binary) stellar evolution (and feedback) with the AMUSE framework (Pelupessy et al., 2013), see e.g., the TORCH project (Wall et al., 2019, 2020) and Reinoso et al. (2023)

Overview of Pop III BBH mergers

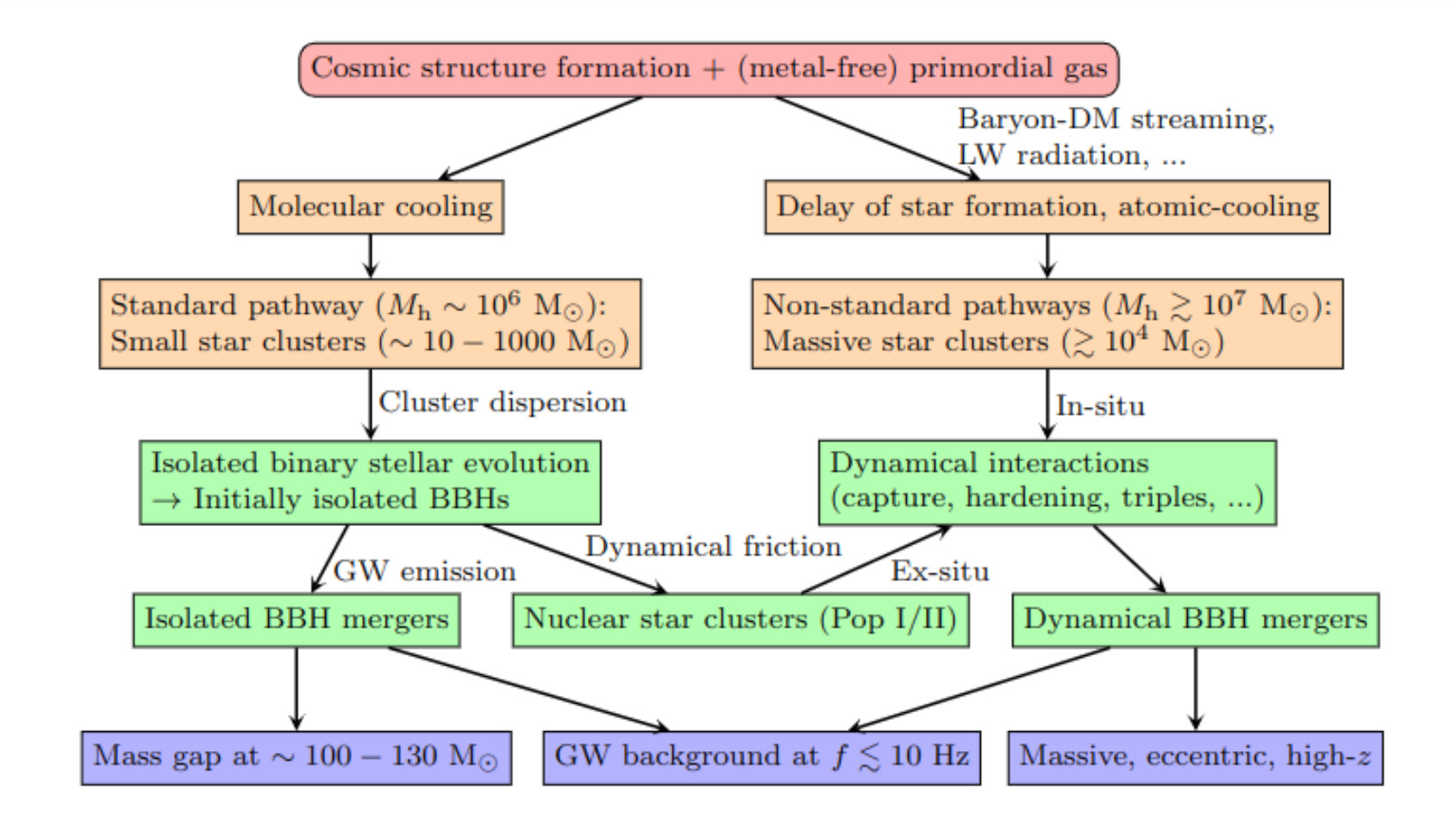

References I

Abbott R., et al., 2020, Phys. Rev. Lett., 125, 101102

Abbott R., et al., 2021, ApJ, 913, L7

Abbott R., et al., 2022a, A&A, 659, A84

Abbott R., et al., 2022b, A& A, 659, A84

Abbott R., et al., 2023, Physical Review X, 13, 011048

Arca-Sedda M., 2016, MNRAS, 455, 35

Arca-Sedda M., Capuzzo-Dolcetta R., 2014, MNRAS, 444, 3738

Bavera S. S., Franciolini G., Cusin G., Riotto A., Zevin M., Fragos T., 2022, A&A, 660, A26

Behroozi P., Wechsler R. H., Hearin A. P., Conroy C., 2019, MNRAS, 488, 3143

Belczynski K., et al., 2016, A&A, 594, A97

Belczynski K., Ryu T., Perna R., Berti E., Tanaka T. L., Bulik T., 2017, MNRAS, 471, 4702

Costa G., Mapelli M., Iorio G., Santoliquido F., Escobar G. J., Klessen R. S., Bressan A., 2023, MNRAS, 525, 2891

Farmer R., Renzo M., de Mink S. E., Marchant P., Justham S., 2019, ApJ, 887, 53

Farrell E., Groh J. H., Hirschi R., Murphy L., Kaiser E., Ekström S., Georgy C., Meynet G., 2021, MNRAS, 502, L40

Finkelstein S. L., 2016, Publ. Astron. Soc. Australia, 33, e037

Franciolini G., Cotesta R., Loutrel N., Berti E., Pani P., Riotto A., 2022, Phys. Rev. D, 105, 063510

References II

Franciolini G., Kritos K., Reali L., Broekgaarden F., Berti E., 2024, arXiv e-prints, p. arXiv:2401.13038

Greif T. H., Bromm V., Clark P. C., Glover S. C., Smith R. J., Klessen R. S., Yoshida N., Springel V., 2012, MNRAS, 424, 399

Hartwig T., et al., 2022, ApJ, 936, 45

Heger A., Fryer C., Woosley S., Langer N., Hartmann D. H., 2003, ApJ, 591, 288

Hijikawa K., Tanikawa A., Kinugawa T., Yoshida T., Umeda H., 2021, MNRAS,

Hirano S., Hosokawa T., Yoshida N., Umeda H., Omukai K., Chiaki G., Yorke H. W., 2014, ApJ, 781, 60

Hirano S., Hosokawa T., Yoshida N., Omukai K., Yorke H. W., 2015, MNRAS, 448, 568

Hirano S., Yoshida N., Sakurai Y., Fujii M. S., 2018, ApJ, 855, 17

Hirano S., Shen Y., Nishijima S., Sakai Y., Umeda H., 2023, MNRAS, 525, 5737

Iorio G., et al., 2023, MNRAS,

Ishiyama T., Sudo K., Yokoi S., Hasegawa K., Tominaga N., Susa H., 2016, ApJ, 826, 9

Iwaya M., Kinugawa T., Tagoshi H., 2023, arXiv e-prints, p. arXiv:2312.17491

Leaman R., van de Ven G., 2022, MNRAS, 516, 4691

Li W., Inayoshi K., Qiu Y., 2021, ApJ, 917, 60

Liu B., Bromm V., 2020a, MNRAS, 495, 2475

Liu B., Bromm V., 2020b, MNRAS, 497, 2839

References III

Liu B., Bromm V., 2021, MNRAS, 506, 5451

Liu B., Meynet G., Bromm V., 2021, MNRAS, 501, 643

Liu S., Wang L., Hu Y.-M., Tanikawa A., Trani A. A., 2023a, arXiv e-prints, p. arXiv:2311.05393

Liu B., Meynet G., Bromm V., 2023b, MNRAS, 522, 446

Liu B., et al., 2024, arXiv e-prints, p. arXiv:2406.17397

Ma L., Hopkins P. F., Ma X., Anglés-Alcázar D., Faucher-Giguère C.-A., Kelley L. Z., 2021, MNRAS, 508, 1973

Madau P., Dickinson M., 2014, ARA&A, 52, 415

Mapelli M., 2020, Formation channels of single and binary stellar-mass black holes. Springer, pp 1–65

Mapelli M., Spera M., Montanari E., Limongi M., Chieffi A., Giacobbo N., Bressan A., Bouffanais Y., 2020, ApJ, 888, 76

Marchant P., Renzo M., Farmer R., Pappas K. M., Taam R. E., De Mink S. E., Kalogera V., 2019, ApJ, 882, 36

Mestichelli B., Mapelli M., Torniamenti S., Arca Sedda M., Branchesi M., Costa G., Iorio G., Santoliquido F., 2024, arXiv e-prints, p. arXiv:2405.06037

Neumayer N., Seth A., Böker T., 2020, A&ARv, 28, 4

Park J., Ricotti M., Sugimura K., 2023, MNRAS, 521, 5334

Park J., Ricotti M., Sugimura K., 2024, MNRAS, 528, 6895

Pelupessy F. I., van Elteren A., de Vries N., McMillan S., Drost N., Zwart S. P., 2013, A&A, 557, A84

References IV

Pillepich A., et al., 2018, MNRAS, 473, 4077

Portegies Zwart S. F., McMillan S. L. W., Gieles M., 2010, ARAA, 48, 431

Reinoso B., Klessen R. S., Schleicher D., Glover S. C. O., Solar P., 2023, MNRAS, 521, 3553

Sana H., et al., 2012, Science, 337, 444

Santoliquido F., Mapelli M., Iorio G., Costa G., Glover S. C. O., Hartwig T., Klessen R. S., Merli L., 2023, MNRAS,

Santoliquido F., et al., 2024, arXiv e-prints, p. arXiv:2404.10048

Schauer A. T. P., Drory N., Bromm V., 2020, ApJ, 904, 145

Somerville R. S., et al., 2018, MNRAS, 473, 2714

Stacy A., Bromm V., 2013, MNRAS, 433, 1094

Stacy A., Greif T. H., Klessen R. S., Bromm V., Loeb A., 2013, MNRAS, 431, 1470

Sugimura K., Matsumoto T., Hosokawa T., Hirano S., Omukai K., 2020, ApJ, 892, L14

Sugimura K., Matsumoto T., Hosokawa T., Hirano S., Omukai K., 2023, ApJ, 959, 17

Susa H., 2019, ApJ, 877, 99

Tanikawa A., 2024, Reviews of Modern Plasma Physics, 8, 13

Tanikawa A., Kinugawa T., Yoshida T., Hijikawa K., Umeda H., 2021a, MNRAS, 505, 2170

Tanikawa A., Susa H., Yoshida T., Trani A. A., Kinugawa T., 2021b, ApJ, 910, 30

References V

Tanikawa A., Yoshida T., Kinugawa T., Trani A. A., Hosokawa T., Susa H., Omukai K., 2022, ApJ, 926, 83

Torniamenti S., Pasquato M., Di Cintio P., Ballone A., Iorio G., Artale M. C., Mapelli M., 2022, MNRAS, 510, 2097

Wall J. E., McMillan S. L. W., Mac Low M.-M., Klessen R. S., Portegies Zwart S., 2019, ApJ, 887, 62

Wall J. E., Mac Low M.-M., McMillan S. L. W., Klessen R. S., Portegies Zwart S., Pellegrino A., 2020, ApJ, 904, 192

Wang L., Tanikawa A., Fujii M., 2022, MNRAS, 515, 5106

Woosley S., 2017, ApJ, 836, 244

Yi S.-X., Nelemans G., Brinkerink C., Kostrzewa-Rutkowska Z., Timmer S. T., Stoppa F., Rossi E. M., Portegies Zwart S. F., 2022a, A&A, 663, A155

Yi S.-X., Stoppa F., Nelemans G., Cator E., 2022b, A&A, 663, A156